Research Square

Preprints are preliminary reports that have not undergone peer review.
They should not be considered conclusive, used to inform clinical practice,
or referenced by the media as validated information.

Divergent fasting lactate responses are associated with serum multi-omics remodelling after 14-week high-intensity interval training in type 2 diabetes

Jiuxiang Gao
Shanghai Jiao Tong University
Yuchen Wang
Shanghai Jiao Tong University
Hui Zuo
Shanghai Jiao Tong University
Xiaohui Liu
Shanghai Jiao Tong University
Tao Zhang
Shanghai Jiao Tong University
Ngai Choi
Shanghai Jiao Tong University
Chuanzhi Wang
South China Normal University
Tianxiao Guo
Shanghai Jiao Tong University
Xinfei Wen
Donghua University
Weiliang Xia
Shanghai Jiao Tong University
Jingyan Tian
Ruijin Hospital
Kang Chen
Shanghai Jiao Tong University
Qingwei Lu
Jiangchuan Community Health Service Center
Liang Yu
Beijing Sport University
Xiuqiang Wang
Shanghai Jiao Tong University
Kun Qian
Shanghai Jiao Tong University
Sulin Cheng
sulin.cheng@jyu.fi

University of Jyväskylä

Study protocol

Keywords: Type 2 diabetes mellitus, Fasting lactate, High-intensity interval training, Exercise adaptation, lactate response divergent, Metabolomics, Proteomics, Precision exercise medicine

Posted Date: July 7th, 2026

DOI: https://doi.org/10.21203/rs.3.rs-10191139/v1

License: This work is licensed under a Creative Commons Attribution 4.0 International License. Read Full License

Additional Declarations: Competing interest reported. Professor Jingyan Tian, a co-author of this manuscript, is serving as a Guest Editor for this Collection. We respectfully request that the manuscript be handled independently according to the journal's editorial policy, without her involvement in the editorial assessment or peer-review process.

Abstract

Background

Type 2 diabetes mellitus (T2DM) is characterised by impaired glucose regulation, insulin resistance and altered substrate metabolism. Exercise training improves glycaemic control and cardiorespiratory fitness, but individual metabolic adaptation remains heterogeneous. We investigated whether fasting lactate response after chronic exercise identifies distinct clinical and serum multi-omics remodelling patterns in T2DM.

Methods

This study included an independent baseline validation cohort and a 14-week supervised exercise intervention cohort. In the baseline cohort, fasting lactate, clinical markers and serum metabolomic profiles were compared between non-T2DM controls and patients with T2DM. In the intervention cohort, patients with T2DM completed rowing-based high-intensity interval training (HIIT), with fasting lactate assessed at baseline, week 7 and week 14. Exercised participants were classified according to tertiles of 0–14-week lactate change into lactate-decreased (LD), lactate-maintained (LM) and lactate-increased (LI) groups. Clinical markers, continuous glucose monitoring (CGM) profiles, untargeted serum metabolomics and serum proteomics were analysed.

Results

At baseline, patients with T2DM had higher fasting lactate than non-T2DM controls (1.72 ± 0.70 vs. 1.06 ± 0.57 mmol/L; $P < 0.001$, false discovery rate < 0.001), accompanied by impaired glucose–insulin homeostasis and exploratory metabolomic differences. During training, fasting lactate showed marked inter-individual heterogeneity. From baseline to week 14, lactate decreased in LD (− 1.08 ± 1.20 mmol/L), remained relatively stable in LM (+ 0.09 ± 0.21 mmol/L) and increased in LI (+ 1.15 ± 0.60 mmol/L), whereas the non-exercise control group showed minimal change (− 0.04 ± 0.79 mmol/L). The 0–14-week lactate change differed markedly between LD and LI ($P < 0.001$), and baseline lactate was inversely associated with subsequent lactate change ($\rho = -0.63$, $P < 0.001$). Fasting glucose, CGM profiles and peak oxygen uptake improved across trained groups. However, LI showed unfavourable trends in fasting insulin, HOMA-IR and triglyceride responses. Exploratory serum metabolomics linked lactate response to lipid- and redox-related features, including phospholipid, sphingolipid, acylcarnitine and fatty-acid handling modules, with PI (17:0/14:1(9Z)) emerging as the strongest adjusted candidate. Exploratory proteomics further highlighted lipid/adipokine, immune/complement, extracellular remodelling and cellular stress/RNA-related features.

Conclusions

Fasting lactate was elevated in T2DM and showed heterogeneous adaptation after 14 weeks of HIIT. Lactate-response groups captured a metabolic dimension not fully reflected by conventional glycaemic improvement. Exploratory metabolomic and proteomic findings suggest multi-layered substrate-handling, redox-related and systemic remodelling signatures associated with divergent lactate responses, warranting targeted validation in larger cohorts.

Trial registration:

Chinese Clinical Trial Registry, ChiCTR-IOR-16008469.

Research Insights

What is currently known about this topic?	Exercise training improves glycaemic control, insulin sensitivity and cardiometabolic health in patients with T2DM.
	Lactate is increasingly recognized as a carbon shuttle and metabolic signal, not merely a metabolic waste product.
	Exercise responses vary substantially in T2DM, yet fasting lactate is rarely used to stratify adaptation.
What is the key research question?	Can fasting lactate response distinguish clinical and serum multi-omics adaptation after chronic HIIT in T2DM?
What is new?	Patients with T2DM had higher fasting lactate, with lactate-linked serum metabolomic differences.
	Fasting lactate responses diverged after exercise, revealing metabolic heterogeneity beyond glycaemia.
	The lactate-increased group showed adverse insulin, triglyceride and lipid/redox-omics responses.
How might this study influence clinical practice?	Fasting lactate may help identify residual adverse insulin and lipid responses after chronic exercise in T2DM.

Background

Type 2 diabetes mellitus (T2DM) is a complex metabolic disease with systemic cardiometabolic consequences [1, 2]. It is characterised not only by chronic hyperglycaemia, but also by insulin resistance, impaired substrate utilisation, mitochondrial metabolic stress and increased cardiovascular risk [3]. Exercise training is a cornerstone strategy for T2DM management and is commonly implemented alongside standard pharmacological therapy, including metformin [4–6]. Regular physical activity improves glycaemic control, insulin sensitivity, cardiorespiratory fitness and cardiometabolic risk profiles [4, 5], while metformin remains a first-line pharmacological therapy with broad effects on hepatic glucose production [6, 7], mitochondrial function, cellular redox state and energy metabolism [8]. However, individual responses to exercise training under these therapeutic backgrounds are heterogeneous, and the biological factors underlying divergent exercise adaptation in patients with T2DM remain incompletely understood.

Lactate has traditionally been viewed as a marker of anaerobic glycolysis or metabolic stress, but this interpretation is increasingly insufficient. Contemporary evidence indicates that lactate is a major circulating carbon carrier, oxidative substrate and signalling metabolite that links glycolytic flux with mitochondrial oxidation, gluconeogenesis, redox balance and inter-organ substrate exchange [9–11]. Human tracer studies further show that lactate shuttling contributes substantially to postprandial carbohydrate carbon distribution even under aerobic conditions, suggesting that circulating lactate reflects broader metabolic flux rather than hypoxia alone [12]. This concept is particularly relevant in T2DM, where impaired metabolic flexibility, altered pyruvate handling, mitochondrial redox imbalance and metformin-related modulation of lactate-derived gluconeogenesis may jointly influence lactate homeostasis [7, 8, 11].

Exercise-induced adaptation extends beyond glycaemic control alone. Recent metabolomic and multi-omic studies have shown that T2DM and its cardiovascular complications are accompanied by disturbances in pathways related to energy production, substrate utilisation, amino acid metabolism, lipid handling and mitochondrial function [13–15]. These pathways are closely linked to insulin resistance and cardiometabolic risk [14–16]. Because lactate production, oxidation and inter-organ shuttling are tightly coupled to glycolytic flux, mitochondrial oxidative metabolism and substrate availability, exercise-induced changes in fasting lactate may reflect systemic metabolic adaptation rather than an isolated change in circulating lactate concentration.

Despite these advances, several important gaps remain. First, most exercise studies in T2DM focus on average changes in glucose, HbA1c, insulin resistance or body composition, whereas heterogeneity in lactate adaptation after long-term training

has received limited attention. Second, it remains unclear whether patients with T2DM exhibit uniform fasting lactate responses to structured exercise training or whether distinct lactate-response groups can be identified. Third, the serum metabolomic and proteomic remodelling associated with divergent lactate adaptation remains poorly understood, particularly in relation to substrate competition and metabolic flexibility across carbohydrate, amino acid and lipid pathways. Finally, fasting lactate may already differ between patients with T2DM and non-T2DM controls before exercise intervention, potentially reflecting altered glucose–lactate metabolism and medication-related influences, including metformin. Because both exercise intervention and metformin are central components of T2DM management, this baseline context is clinically relevant for interpreting heterogeneous lactate adaptation after exercise training.

In this study, we first compared fasting lactate levels and serum metabolomic profiles between non-T2DM controls and patients with T2DM to define the baseline lactate-associated metabolic background. We then examined fasting lactate trajectories during a 14-week supervised rowing-based high-intensity interval training (HIIT) intervention and classified patients with T2DM into lactate-response groups according to the 0–14-week change in fasting lactate. Finally, using paired serum metabolomics and proteomics, we characterised exploratory molecular remodelling across selected metabolic axes related to central carbon/TCA metabolism, redox balance, amino acid/pyruvate-related metabolism, glycation-related metabolism, dicarboxylate/ω-oxidation-associated fatty-acid handling and systemic proteomic remodelling. We hypothesised that chronic HIIT would reveal divergent fasting lactate responses in T2DM and that these responses would be accompanied by distinct substrate-handling and systemic proteomic signatures rather than reflecting changes in lactate concentration alone.

Methods

Study design

This longitudinal exercise intervention study was conducted in an outpatient clinical setting at the Exercise Translational Medicine Centre, Shanghai Jiao Tong University, China. Participants were recruited from Jiangchuan Community Health Service Centre, Minhang District, Shanghai. The overall study protocol is shown in Fig. 1A.

Participants

Eligible participants were men and women aged 30–65 years with diagnosed T2DM, body mass index (BMI) > 24 kg/m², and a history of treatment with metformin alone or metformin combined with an α-glucosidase inhibitor. The maximum prescribed daily dose of metformin was 2000 mg, with possible dosing regimens including 500 mg three times daily, 850 mg twice daily, or 1000 mg twice daily. Eligible participants had used glucose-lowering medication for no more than 5 years.

Participants were excluded if they had BMI > 38 kg/m², severe cardiovascular disease, severe musculoskeletal disease, type 1 diabetes, psychological disorders, or current insulin therapy. An additional safety exclusion criterion of fasting blood glucose > 16.0 mmol/L was applied where appropriate.

A total of 201 participants entered the recruitment process for the exercise intervention study, of whom 81 met the eligibility criteria. Ultimately, 60 participants agreed to participate, and 53 completed the final study assessments. Among these participants, 40 completed the 14-week supervised exercise training intervention, while 13 patients with T2DM who did not undergo exercise training served as the non-exercise T2DM control group.

The trial was registered in the Chinese Clinical Trial Registry (ChiCTR-IOR-16008469). The study was conducted in accordance with the Declaration of Helsinki and was approved by the Ethics Committee of Shanghai Jiao Tong University (approval numbers: ML16027 and B2020023I). All participants provided written informed consent before enrolment. The original registered trial planned to recruit 280 participants; however, recruitment and intervention delivery were affected by the COVID-19 pandemic. Therefore, the present analysis was based on the available subset with complete longitudinal lactate and omics-related data and focused on lactate metabolism and exercise adaptation.

Independent baseline cohort for cross-sectional comparison

Because the longitudinal exercise intervention included only patients with T2DM, it could not determine whether fasting lactate concentrations and serum metabolomic profiles already differed between individuals with and without T2DM. We therefore used an independent baseline cohort from another study conducted by the principal investigator's group [17–19]. Participants who attended both screening and baseline assessments and had available baseline clinical and metabolomic data were included. Patients with T2DM were identified according to clinical history and/or oral glucose tolerance test results. Age-matched individuals without T2DM served as non-T2DM controls.

This baseline comparison included 232 non-T2DM controls aged 48–67 years (58 men [25.0%] and 174 women [75.0%]) and 120 patients with T2DM aged 49–66 years (25 men [20.8%] and 95 women [79.2%]). The study protocol is shown in Fig. 1B.

Demographic, lifestyle and anthropometric assessments

Baseline demographic characteristics, medication history and lifestyle information were collected using questionnaires. Physical activity was assessed according to leisure-time physical activity intensity, exercise duration per session and exercise frequency per week. Sedentary behaviour was assessed as daily sedentary time, calculated as sitting or reclining hours plus sitting or reclining minutes divided by 60. Dietary information was collected using weekly food-frequency records. Smoking status was recorded as a binary variable, classified as yes or no. Body weight and height were measured using standard procedures. BMI was calculated as body weight in kilograms divided by height in metres squared.

Body composition assessment

Whole-body fat mass, lean mass and body fat percentage, as well as android and gynoid fat mass, were assessed using dual-energy X-ray absorptiometry (Hologic Inc, Bedford, MA). The precision of repeated dual-energy X-ray absorptiometry measurements, expressed as the coefficient of variation, was 0.89% for whole-body fat mass, 0.51% for lean mass and 2.75% for the android-to-gynoid fat distribution ratio[20].

Cardiopulmonary exercise testing

At baseline and week 14, participants underwent cardiopulmonary exercise testing to assess peak oxygen uptake (VO_2peak) and aerobic fitness. Tests were performed on a magnetic-resistance rowing ergometer (DOMYOS 500, Decathlon, France). Participants wore a portable cardiopulmonary exercise testing system (K4b2, Cosmed, Italy) and a heart-rate monitor (Polar H10, Polar, Finland) for continuous measurement of oxygen uptake, carbon dioxide production, respiratory exchange ratio and heart rate.

Before the test, participants completed a 5-min warm-up on the rowing ergometer. The graded rowing test then started at resistance level 1. Rowing resistance was increased by one level every 2 min, up to a maximum of level 15, until volitional exhaustion, completion of the highest resistance level or the occurrence of symptoms requiring test termination. Participants were instructed to maintain a rowing cadence of 26 strokes/min using a metronome throughout the test. At the end of each workload stage and at test termination, resistance level, heart rate and rating of perceived exertion on the Borg 6–20 scale were recorded. The test was terminated immediately if participants developed contraindications or symptoms according to American College of Sports Medicine exercise-testing safety criteria[21].

The highest oxygen uptake achieved during the graded rowing test was recorded as VO_2peak and was calculated as the highest 30-s averaged value. If a clear oxygen uptake plateau was not observed, the highest oxygen uptake attained during the test was used as peak oxygen uptake. A valid near-maximal effort was confirmed when at least two of the following criteria were met: heart rate ≥ 90% of age-predicted maximal heart rate, calculated as 0.90 × (220 − age); rating of perceived exertion > 17; respiratory exchange ratio ≥ 1.15; or blood lactate concentration > 8 mmol/L.

Blood lactate and glucose concentrations were measured at rest, immediately after exercise and at 5, 10 and 30 min during recovery to evaluate exercise-induced metabolic responses and post-exercise recovery.

Exercise intervention

Participants in the exercise intervention group completed a 14-week supervised rowing-based high-intensity interval training intervention. Training was performed three times per week, with at least one day between two consecutive sessions. All sessions were conducted on a magnetic-resistance rowing ergometer (DOMYOS 500, Decathlon, France) and supervised by trained staff throughout the intervention period.

Exercise intensity was individually prescribed according to each participant's maximal rowing workload, which was determined from the graded rowing workload assessment described above. The maximal workload measured at baseline was used to prescribe training intensity during weeks 1–7. At week 7, maximal rowing workload was reassessed, and the exercise prescription was adjusted accordingly for weeks 8–14.

During weeks 1–7, each session consisted of a 5-min warm-up, repeated intervals alternating between 3 min of low-intensity rowing at approximately 40% of maximal workload and 1 min of high-intensity rowing at approximately 90% of maximal workload, followed by a 5-min cool-down. During weeks 8–14, the intervention was progressed by shortening the low-intensity recovery intervals to 2 min, while maintaining the high-intensity intervals at approximately 90% of the reassessed maximal workload.

Participants were instructed to consume breakfast or lunch approximately 30–60 min before the scheduled exercise session. Participants in the non-exercise T2DM control group were instructed to maintain their usual diet and physical activity habits and not to undertake additional structured exercise during the study period.

Blood collection and biochemical analyses

Venous blood samples were collected in the morning between 07:00 and 08:30 after an overnight fast. Serum or plasma was separated by centrifugation and stored at − 80°C until analysis where appropriate. Whole-blood samples were used for haematological measurements, HbA1c analysis and lactate assessment. Inter- and intra-assay coefficients of variation (CVs) were 1.0% and 1.1% for HbA1c, < 5.0% and < 8.5% for lactate, respectively.

Haematological parameters, including haemoglobin, white blood cell count, red blood cell count, haematocrit, erythrocyte indices, platelet indices and leukocyte differentials, were measured using an automated haematology analyser. Glucose, triglycerides, total cholesterol (TC), high-density lipoprotein cholesterol (HDL-C) and low-density lipoprotein cholesterol (LDL-C) were measured using enzymatic methods on an automated biochemical analyser (AU680, Beckman Coulter, USA). HbA1c was measured using an automated glycohaemoglobin analyser (H50, Mindray, China). Insulin and C-peptide were measured using electrochemiluminescence immunoassays on an automated immunoassay analyser (Cobas e602, Roche, Switzerland). Venous whole-blood lactate concentration was measured using a portable blood lactate analyser and corresponding test strips (Lactate Pro 2 LT-1730, Arkray, Japan). Inter- and intra-assay coefficients of variation (CVs) were 2.0% and 3.7% for glucose, 11.0% and 3.4% for insulin, 1.0% and 1.0% for triglycerides, 1% and 1.0% for TC, 1% and 1.2% for HDL-C, and 2% and 2.2% for LDL-C, respectively.

A standard oral glucose tolerance test was performed after an overnight fast of at least 10 h. After a fasting blood sample was obtained, participants ingested 75 g anhydrous glucose dissolved in water. Venous blood samples were collected at 30 and 120 min after glucose ingestion. Glucose, insulin and C-peptide responses during the oral glucose tolerance test were used to evaluate glucose tolerance, early insulin response and insulin-related metabolic status.

Insulin resistance was estimated using the homeostasis model assessment of insulin resistance:

HOMA-IR = fasting glucose mmol/L × fasting insulin μIU/mL / 22.5 [22].

In the exercise intervention cohort, fasting insulin sensitivity was represented using a reciprocal HOMA-derived insulin sensitivity index, calculated as 100/HOMA-IR. Higher 100/HOMA-IR values indicate greater fasting insulin sensitivity.

Whole-body insulin sensitivity was additionally estimated using a modified Matsuda insulin sensitivity index:

ISI-M = 10,000 / √[(G0 × I0) × (Gmean × Imean)][23],

where G0 and I0 represent fasting glucose and fasting insulin, respectively, and Gmean and Imean represent time-weighted mean glucose and insulin concentrations during the OGTT. Because glucose was measured in mmol/L, glucose values were converted to mg/dL by multiplying by 18.018 before ISI-M calculation. Higher ISI-M values indicate greater insulin sensitivity.

Continuous glucose monitoring

In the exercise intervention protocol, all participants used a continuous glucose monitoring (CGM) system (FreeStyle Libre H; Abbott Diabetes Care, UK). The sensor was worn on the lateral upper arm for up to 14 consecutive days and continuously monitored interstitial glucose concentrations. Historical glucose readings were stored at 15 min intervals and retrieved by scanning the sensor.

Each participant underwent CGM assessment during two separate periods. The first monitoring period started at the beginning of the exercise intervention, and the second monitoring period was conducted during the final 14 days before completion of the 14-week intervention. For each monitoring period, data from the first 2 days and the last 2 days were excluded to minimize potential sensor instability and incomplete recording effects. The remaining 10 days of data were used to generate standard-day CGM profiles before and after the intervention.

Standardised CGM metrics for clinical care were calculated from the standard-day CGM profiles according to international consensus recommendations and the ADA Standards of Care for diabetes technology [24, 25]. These included mean glucose, maximum standard-day glucose, minimum standard-day glucose, glucose excursion, calculated as maximum glucose minus minimum glucose, glycaemic variability expressed as the coefficient of variation (CV), percentage of time above range (TAR; >10.0 mmol/L[> 180 mg/dL]), and percentage of time in range (TIR; 3.9–10.0 mmol/L[70–180 mg/dL]).

Serum metabolomic profiling and preprocessing

Serum metabolomic profiling was performed using two untargeted LC–MS workflows according to the study component. Because the independent baseline case-control cohort and the longitudinal exercise intervention cohort were profiled using different sample-preparation procedures and mass spectrometry platforms, metabolomic results were analysed within each cohort-specific framework and were not directly compared at the raw feature-abundance level.

For the baseline case-control cohort, serum samples were stored at − 80°C and thawed on ice before extraction. Polar metabolites were extracted by adding 50 μL serum to an Ostro solid-phase extraction plate (Waters, Milford, MA, USA), followed by 150 μL acetonitrile containing 0.1% formic acid. The flow-through was collected using a positive-pressure processor, and each well was washed twice with 50 μL acetonitrile containing 0.1% formic acid. The collected fractions were combined as the polar metabolite extract. Untargeted serum polar metabolomic profiling was performed using an Acquity UPLC I-class system coupled to a VION IMS Q-TOF mass spectrometer (Waters), with separation on an HSS T3 C18 column and data acquisition in MSE mode under both positive- and negative-ion electrospray ionization.

For the longitudinal exercise intervention cohort, serum samples collected at baseline, week 7 and week 14 were stored at − 80°C until analysis. For metabolite extraction, 50 μL serum was mixed with 200 μL methanol/acetonitrile (1:1, v/v; HPLC grade) containing 2 μg/mL chlorophenylalanine as the internal standard. Samples were vortexed, incubated at − 20°C for 2 h and centrifuged at 12,000 rpm for 20 min at 4°C. The supernatant was dried under vacuum, reconstituted in methanol/water (3:7, v/v), transferred to sample vials and stored at − 20°C before LC–MS analysis. Pooled quality-control samples and blank

samples were processed in parallel. Untargeted serum metabolomic profiling was performed using a Q Exactive Plus Orbitrap LC–MS/MS system (Thermo Fisher Scientific).

Raw LC–MS data from both workflows were processed using the same general Progenesis QI workflow, including peak detection, retention-time alignment, isotope/adduct deconvolution where applicable, intensity preprocessing, normalization, feature annotation and quality-control assessment. Positive- and negative-ion feature matrices were exported separately for downstream analysis. Metabolite features were annotated by matching against public databases, including the Human Metabolome Database and METLIN, with LIPID MAPS queried where applicable for lipid-related annotations. Analyses were performed at the QC-filtered LC–MS feature level, and putative metabolite names were retained only as display annotations. Within each cohort, positive- and negative-ion features were processed separately and then stacked as unmerged feature-level tables; candidate cross-mode duplicates were not collapsed by metabolite name. Features were retained if they met predefined QC criteria, including QC coefficient of variation ≤ 30%, sample detection ratio ≥ 0.50 and maximum abundance ≥ 500 for the baseline cohort or ≥ 1000 for the longitudinal intervention cohort, where available. Sample-level data structure and post-preprocessing signal distributions were inspected using principal component analysis and median-centred feature-level z-score boxplots (Fig. S1).

Serum proteomic profiling and preprocessing

Serum proteomic profiling was performed using a data-independent acquisition mass spectrometry workflow. Serum samples were processed using a Deep Sample Preparation kit (OSFP0002; Shanghai Omicsolution Co., Ltd., China), including low-abundance protein enrichment, protein denaturation, reduction, alkylation, Lys-C/trypsin digestion and C18 peptide desalting. Dried peptides were stored at − 80°C until LC–MS/MS analysis. Data acquisition was carried out on an Orbitrap Astral paltform with a 14-min gradient liquid chromotography separation.

Raw DIA-MS/MS data were processed using Spectronaut 20 software (Biognosys AG, Switzerland) with default settings against the UniProt Homo sapiens database, version 2025. Trypsin was specified as the digestion enzyme. Carbamidomethylation of cysteine was set as a fixed modification, and oxidation of methionine and acetylation of the protein N-terminus were set as variable modifications. Precursor, peptide and protein identifications were controlled at a 1% false discovery rate. Protein group quantities were calculated using the MaxLFQ method after local normalization.

For downstream analysis, the processed long-term serum proteomics log2 matrix was used without reprocessing the raw mass spectrometry data. Analyses were performed at the protein feature level using stable protein feature IDs, and gene symbols were used only as display labels. Protein features were retained if they passed protein-level q-value filtering, were not annotated as contaminants and had a protein detection ratio ≥ 0.50. Missing values were retained for paired and association analyses, and row-median imputation was used only for principal component analysis-based quality-control visualization. Protein-level data structure and post-preprocessing abundance distributions were further inspected using principal component analysis and median-centred protein z-score boxplots (Fig. S1).

Batch-related technical variation was evaluated during omics quality control using PCA and sample-distribution diagnostics generated from feature-wise standardized matrices. Platform-specific filtering was applied before downstream modelling. For metabolomics, acquisition batch and injection-order metadata were unavailable in the analysis-ready files. Analyses therefore used vendor-provided $\log_2$ median-normalized matrices with QC-CV, detection-rate and abundance-based filtering. Molecular associations were interpreted as exploratory and evaluated alongside QC diagnostics rather than as formally batch-corrected effects. For proteomics, run-order metadata suggested a technical component, but run order was confounded with longitudinal time point. Empirical batch correction using methods such as ComBat or SVA was therefore not applied in the primary analyses, as this could remove true time-associated biological variation.

Definition of lactate-response phenotypes

For the longitudinal exercise intervention analysis, fasting lactate response was defined as the change in fasting lactate concentration from baseline to week 14:

Δlactate = lactate at week 14 − lactate at baseline.

Patients with T2DM in the exercise intervention group were ranked according to Δlactate and divided into tertiles. Participants in the lowest tertile, representing the greatest reduction in fasting lactate, were classified as the lactate decreased group (LD; n = 13; 5 men and 8 women). Participants in the middle tertile, representing relatively stable fasting lactate, were classified as the lactate maintained group (LM; n = 14; 6 men and 8 women). Participants in the highest tertile, representing the greatest increase in fasting lactate, were classified as the lactate increased group (LI; n = 13; 9 men and 4 women). The 13 non-exercise patients with T2DM served as the Control group (7 men and 6 women) and were not included in the definition of tertile cut-offs.

Statistical analysis

Continuous variables are presented as mean ± standard deviation, median with interquartile range, or individual values, as appropriate. Categorical variables are presented as n (%). Baseline comparisons between two groups were performed using Wilcoxon rank-sum tests for continuous variables and chi-square or Fisher's exact tests for categorical variables, where appropriate. Comparisons across more than two lactate-response phenotypes were performed using Kruskal–Wallis tests, followed by pairwise comparisons where appropriate. Paired comparisons were performed using paired t-tests or Wilcoxon signed-rank tests, depending on data distribution.

Because the present analysis was an exploratory lactate-response and omics sub-study within the registered trial, sample-size adequacy was assessed for the primary longitudinal within-participant lactate-change analysis. Using G*Power 3.1 for a two-sided paired comparison with $\alpha = 0.05$, power = 0.80 and an a priori moderate effect size of Cohen's $dz = 0.50$, a minimum of 34 participants was required. The exercise intervention cohort included 40 participants and therefore met this minimum requirement. Phenotype-stratified omics analyses were considered exploratory.

For the longitudinal exercise intervention analysis, individual Δlactate values were visualised using a waterfall plot. Longitudinal lactate trajectories were analysed using mixed-effects models, with time, lactate-response phenotype and the time-by-phenotype interaction included as fixed effects, and participant ID included as a random intercept. Because lactate-response phenotypes were defined according to the 0–14-week change in fasting lactate, between-phenotype differences in lactate trajectories were interpreted as descriptive confirmation of the phenotype definition rather than as independent validation.

For omics analyses, the main biological readout was the continuous adjusted 14-week lactate response. LD, LM and LI were used as display groups to visualize decreased, maintained and increased lactate-response patterns. For each metabolite feature, week-14 lactate was modelled as a function of baseline lactate, age and standardised 0–14-week metabolite feature change among intervention participants: Lactate_14w ~ Lactate_0w + Age + Molecular_Delta_Z. For each protein feature, week-14 lactate was modelled as a function of baseline lactate, available covariates and standardised 0–14-week protein change: Lactate_14W ~ Lactate_0W + available covariates + Protein_Delta_Z. Available proteomic covariates included age, sex, BMI and drug-class count when non-missing and non-invariant.

For each molecular feature, incremental R^2 was calculated as the difference between the full model R^2 and the base model R^2 without the molecular feature. Endpoint candidates were ranked by nominal P value and incremental R^2, and Benjamini–Hochberg false discovery rate values were retained in the source tables. Descriptive LD–LI contrasts at baseline, week 7 and week 14 were performed using Welch tests on log2 feature abundance and were used for display-level visualization rather than primary inference. Volcano highlighting used nominal $P < 0.05$ and absolute log2 fold-change > 0.5.

A lactate-centred 0W–response–14W association network was constructed to summarize selected clinical, metabolomic and proteomic associations around fasting lactate at baseline, adjusted lactate response over 0–14 weeks and fasting lactate at week 14. Clinical and molecular associations were assessed using time-layer-specific models, including baseline, response-level and endpoint models adjusted for relevant covariates where applicable. Nodes represented clinical indices, metabolite features, protein features and manually curated functional modules. Edges denoted predefined evidence classes, including

lactate-axis links, lactate associations, module-feature membership, repeated features across time layers and prior pathway support, rather than unconstrained network discovery. Node colour indicated beta direction, node size reflected incremental R^2 where applicable, and node border indicated evidence strength.

Benjamini–Hochberg false discovery rate correction was applied within prespecified analysis families. Molecular and network findings were interpreted as exploratory unless they survived the relevant false discovery rate correction; no causal mediation, prediction model or validated biomarker panel was claimed.

Results

Baseline lactate-associated metabolic disturbances in patients with T2DM

We first examined whether fasting lactate was altered in patients with T2DM before the exercise intervention. Compared with non-T2DM controls, patients with T2DM had significantly higher fasting lactate concentrations (1.72 ± 0.70 vs. 1.06 ± 0.57 mmol/L; $P < 0.001$, FDR < 0.001; Fig. 2A). This lactate elevation occurred alongside impaired glucose-insulin homeostasis, including higher HbA1c, fasting glucose, 30-min post-load glucose, 120-min post-load glucose and HOMA-IR, and lower insulin sensitivity index values (all $P < 0.001$; Fig. 2A; Table 1). Patients with T2DM also showed higher fasting and 120-min post-load insulin concentrations, but lower 30-min post-load insulin concentrations, indicating impaired early insulin response with delayed compensatory insulin secretion (all FDR < 0.001; Fig. 2A; Table 1).

Table 1
Baseline characteristics of non-T2DM controls and patients with T2DM

Characteristic	Control	T2DM	P value	FDR
Basic information				
Age (years)	60.2 ± 4.1	59.9 ± 4.2	0.456	0.563
Male/Female, n (%)	58 (25)/174 (75)	25 (21)/95 (79)	0.373	0.530
Height (cm)	162 ± 7.6	160 ± 7.9	0.011	0.023
Weight (kg)	65.6 ± 10.1	67.0 ± 11.2	0.405	0.536
BMI (kg/m2)	25.0 ± 3.2	26.2 ± 3.4	0.002	0.005
Waist circumference (cm)	86.0 ± 8.1	89.1 ± 9.4	0.002	0.005
Hip circumference (cm)	96.5 ± 6.7	98.6 ± 8.1	0.008	0.017
Systolic blood pressure (mmHg)	132 ± 15.3	137 ± 18.4	0.061	0.119
Diastolic blood pressure (mmHg)	82.1 ± 11.3	82.4 ± 9.2	0.447	0.563
Body composition				
Fat mass (kg)	24.7 ± 5.2	24.3 ± 5.5	0.703	0.743
Fat (%)	37.8 ± 5.0	36.7 ± 5.0	0.227	0.353
Lean mass (kg)	38.5 ± 5.7	39.8 ± 8.2	0.800	0.800
Android fat mass (kg)	2.39 ± 0.6	2.37 ± 0.7	0.517	0.598
Gynoid fat mass (kg)	3.36 ± 0.9	3.28 ± 1.0	0.758	0.779
Clinical biomarkers				
Fasting glucose (mmol/L)	4.81 ± 0.5	6.19 ± 1.1	< 0.001	< 0.001
30-min post-load glucose (mmol/L)	8.90 ± 1.5	11.8 ± 2.2	< 0.001	< 0.001
120-min post-load glucose (mmol/L)	6.00 ± 1.0	11.4 ± 3.8	< 0.001	< 0.001
HbA1c (%)	5.76 ± 0.3	6.91 ± 0.8	< 0.001	< 0.001
Fasting insulin (mU/L)	12.4 ± 5.9	15.3 ± 8.7	< 0.001	0.002
30-min post-load insulin (mU/L)	117 ± 67.2	62.2 ± 43.2	< 0.001	< 0.001
120-min post-load insulin (mU/L)	74.6 ± 55.0	104 ± 66.9	< 0.001	< 0.001
Insulin resistance	2.66 ± 1.3	4.32 ± 2.5	< 0.001	< 0.001
Insulin sensitivity	4.26 ± 2.0	2.94 ± 1.5	< 0.001	< 0.001
Fasting C-peptide (ng/mL)	1.37 ± 0.7	1.77 ± 0.8	< 0.001	< 0.001

Characteristic	Control	T2DM	P value	FDR
Basic information				
30-min post-load C-peptide (ng/mL)	5.51 ± 3.4	3.87 ± 2.1	< 0.001	< 0.001
120-min post-load C-peptide (ng/mL)	5.90 ± 3.0	7.97 ± 5.1	< 0.001	< 0.001
Creatinine (umol/L)	69.3 ± 17.5	61.8 ± 17.6	< 0.001	< 0.001
High-density lipoprotein cholesterol (mmol/L)	1.35 ± 0.5	1.21 ± 0.3	0.008	0.017
Low-density lipoprotein cholesterol (mmol/L)	3.26 ± 0.9	3.37 ± 1.0	0.253	0.375
Triglycerides (mmol/L)	1.98 ± 1.6	2.22 ± 2.0	0.129	0.239
Total cholesterol (mmol/L)	5.42 ± 1.0	5.57 ± 1.1	0.229	0.353
Urea nitrogen (mmol/L)	5.18 ± 1.2	5.34 ± 1.2	0.177	0.311
Follicle-stimulating hormone (mIU/mL)	44.9 ± 28.9	41.4 ± 25.9	0.400	0.536
Lifestyle and Leisure-time physical activity				
Inactive/light/moderate/vigorous, n (%)	55(24)/33(15)/139(61)/1(0)	36(30)/23(19)/60(50)/0	0.194	0.326
Exercise duration per session (min)	39.6 ± 34.9	39.7 ± 40.4	0.560	0.628
Exercise frequency (sessions/week)	4.4 ± 5.3	4.6 ± 7.1	0.476	0.569
Daily sedentary time (h/day)	4.2 ± 2.0	4.4 ± 2.4	0.624	0.680
Smoking, Never /Former /Current, n (%)	186(82)/10(4)/32(14)	98(82)/5(4)/16(13)	0.984	0.984
Highest education level 1/2/3, n (%)	201 (88)/27 (12)/0	103 (87)/15 (12)/1(1)	0.447	0.570
Values are mean ± SD or n (%) unless otherwise indicated.				
P values were calculated using the Wilcoxon rank-sum test for continuous variables and Pearson chi-square or Fisher exact tests for categorical variables.				
FDR values were calculated using the Benjamini-Hochberg procedure across all tested data rows in Table 1.				
Lifestyle, smoking and education variables were available for 228 controls and 119 participants with T2DM.				
OGTT 0 min denotes the fasting sample collected before oral glucose load; 30 and 120 min denote post-load samples.				
HOMA-IR and ISI are derived indices.				
Daily sedentary time was recalculated as sitting/reclining hours plus sitting/reclining minutes/60; the current Baseline_all source does not contain a sleep-duration field.				
Available sample sizes vary by marker; marker-level n values are provided in the source-data workbook.				
Highest education level: 1 = below bachelor's degree; 2 = bachelor's degree; 3 = postgraduate degree.				

In addition, significant between-group differences were observed in height, BMI, waist and hip circumferences, fasting and postprandial C-peptide, creatinine and HDL-C. In contrast, no significant differences were found in age, gender, body weight,

blood pressure, whole-body or regional fat mass, LDL-C, triglycerides, total cholesterol, urea nitrogen, follicle-stimulating hormone, lifestyle factors including leisure-time physical activity and smoking status, or education level (Table 1).

We next assessed whether this elevated basal lactate phenotype was accompanied by broader serum metabolomic remodelling. In the validation metabolomics subset, six quality-control-flagged samples were excluded, leaving 36 controls and 24 patients with T2DM for analysis across 1,267 detected features. Principal component analysis showed partial group separation, while standardised abundance distributions were broadly comparable across samples (Fig. S1A, B). Differential metabolite analysis identified 78 nominally altered features between patients with T2DM and controls, including 27 features with $P < 0.05$ and $|\log2 \text{ fold change}| \geq 0.5$, and nine features with $P < 0.05$ and $|\log2 \text{ fold change}| \geq 1.0$. However, no metabolite features remained significant after global FDR correction (Fig. 2B).

Among the putatively annotated features shown in the forest plot, several metabolites were higher in patients with T2DM, including isomorellic acid (log2 difference = 1.45, P = 0.009), traumatic acid (log2 difference = 1.25, P = 0.009), isamoxole (log2 difference = 0.99, P = 0.011), O-desmethylnaproxen (log2 difference = 0.85, P = 0.03), Testosterone enanthate (log2 difference = 0.76, P = 0.02), Calcitroic acid (log2 difference = 0.77, P = 0.02). Conversely, brainesteroside C (log2 difference = − 1.84, P = 0.022), iodotyrosine (log2 difference = − 1.43, P = 0.010), a phosphatidic acid-like feature (log2 difference = − 1.02, P = 0.025) and hemin (log2 difference = − 0.98, P < 0.001) were lower in patients with T2DM (Fig. 2C).

To place the elevated fasting lactate phenotype in a broader metabolic context, we further visualised a biologically curated panel of metabolites involved in lactate-connected metabolic axes, including central carbon/TCA metabolism, BCAA-related metabolism and dicarboxylate/ω-oxidation-related lipid handling (Fig. 2D). Although these individual metabolites did not show robust between-group significance in this baseline validation dataset, the heatmap was used as an exploratory pathway-guided visualization rather than as a differential metabolite screen. This analysis suggests that elevated basal lactate in T2DM may occur within a broader metabolic background involving altered carbon flux, amino acid metabolism and lipid oxidation-related substrate handling.

Together, these results indicate that fasting lactate was already elevated in patients with T2DM at baseline and was accompanied by impaired glucose-insulin homeostasis and exploratory serum metabolomic differences. This baseline lactate-centred metabolic background provides the rationale for using lactate response as the anchor phenotype in subsequent exercise intervention analyses.

Longitudinal exercise revealed heterogeneous lactate responses in patients with T2DM

We next examined fasting lactate adaptation during the 14-week supervised HIIT intervention. Longitudinal clinical, fitness, rowing performance, standard-day CGM and dietary variables across response groups are summarized in Table 2 and visualized in Fig. 3 and Fig. S2. Baseline and at 14 weeks dietary intakes were also assessed.

Table 2
Exercise intervention-related outcomes across lactate-response groups

Characteristic	Time	Control	LD	LM	LI	Control vs LD	Control vs LM	Control vs LI	LD vs LM	LD vs LI	LM vs LI
Fasting lactate (mmol/L)	0W	1.65 ± 0.74	2.55 ± 1.21	1.35 ± 0.44	1.03 ± 0.38	0.092	0.389	0.020	0.008	0.001	0.071
	7W	2.09 ± 1.42	2.09 ± 0.42	1.62 ± 0.43	1.73 ± 0.49	0.265	0.943	1.000	0.051	0.116	0.846
	14W	1.62 ± 0.90	1.48 ± 0.93	1.44 ± 0.49	2.18 ± 0.59	0.719	0.826	0.005	0.942	0.051	0.002
Fasting glucose (mmol/L)	0W	7.54 ± 1.75	7.71 ± 2.37	7.53 ± 2.41	7.43 ± 2.21	0.878	0.482	0.538	1.000	0.720	0.680
	7W	7.11 ± 1.59	6.67 ± 0.46	7.24 ± 1.47	6.96 ± 0.99	0.791	0.696	0.810	0.583	0.685	0.969
	14W	6.88 ± 1.41	6.54 ± 0.93	7.09 ± 1.91	7.30 ± 1.30	0.608	0.752	0.383	0.396	0.137	0.216
HbA1c (%)	0W	7.17 ± 0.96	7.22 ± 1.22	6.80 ± 1.31	6.56 ± 1.07	0.797	0.099	0.040	0.099	0.045	0.274
	7W	6.87 ± 0.97	7.01 ± 0.87	6.64 ± 0.63	6.58 ± 0.73	0.832	0.301	0.359	0.219	0.246	0.486
	14W	6.67 ± 0.70	6.74 ± 0.61	6.55 ± 0.48	6.34 ± 0.58	0.857	0.593	0.182	0.451	0.117	0.343
Fasting insulin (mU/L)	0W	8.57 ± 5.14	14.5 ± 6.51	10.3 ± 4.99	11.0 ± 3.51	0.020	0.234	0.228	0.094	0.151	0.396
	7W	12.6 ± 10.0	15.9 ± 5.27	10.1 ± 5.75	11.8 ± 5.72	0.203	0.847	0.793	0.047	0.093	0.375
	14W	7.90 ± 4.86	14.5 ± 5.45	9.13 ± 4.14	16.8 ± 11.2	0.006	0.297	0.009	0.011	0.878	0.035
Insulin resistance (index)	0W	3.09 ± 2.28	5.25 ± 3.48	3.31 ± 1.56	3.55 ± 1.35	0.058	0.482	0.259	0.132	0.356	0.645
	7W	4.17 ± 3.48	4.70 ± 1.68	3.35 ± 2.04	3.58 ± 1.48	0.452	0.847	0.875	0.139	0.272	0.616
	14W	2.54 ± 1.92	4.14 ± 1.57	2.93 ± 1.59	5.63 ± 4.77	0.017	0.320	0.021	0.069	0.505	0.055
Insulin sensitivity (100/HOMA-IR)	0W	59.8 ± 55.5	28.3 ± 18.2	37.2 ± 17.4	32.5 ± 13.7	0.058	0.482	0.259	0.132	0.356	0.645
	7W	45.5 ± 37.6	23.9 ± 9.24	47.0 ± 41.4	41.9 ± 44.0	0.452	0.847	0.875	0.139	0.272	0.616
	14W	59.6 ± 35.8	28.2 ± 12.8	55.9 ± 55.8	30.2 ± 26.6	0.017	0.320	0.021	0.069	0.505	0.055

Values are presented as mean ± SD unless otherwise indicated. Measurements are shown at baseline (0W), week 7 (7W) and week 14 (14W).

Pairwise P values compare groups at the same time point. Control denotes the non-exercise T2DM control group; LD, LM and LI denote the lactate-decreased, lactate-maintained and lactate-increased exercise-response groups, respectively.

Standard-day CGM variables were calculated after excluding early and late unstable valid days where possible and summarizing retained stable days using 15-min median glucose profiles.

Dietary intake sample sizes varied by group and time point; values with zero SD reflect limited available observations.

Characteristic	Time	Control	LD	LM	LI	Control vs LD	Control vs LM	Control vs LI	LD vs LM	LD vs LI	LM vs LI
Total cholesterol (mmol/L)	0W	5.03 ± 1.38	5.00 ± 1.47	5.01 ± 1.31	4.80 ± 0.59	0.758	0.680	0.644	0.923	1.000	0.610
	7W	4.86 ± 0.93	5.26 ± 1.05	5.29 ± 1.15	5.08 ± 0.69	0.459	0.201	0.847	1.000	0.685	0.375
	14W	4.64 ± 1.08	4.61 ± 1.28	4.88 ± 1.26	4.78 ± 0.60	0.837	0.482	0.608	0.467	0.538	0.884
Triglycerides (mmol/L)	0W	2.30 ± 1.75	1.70 ± 0.65	1.58 ± 1.05	2.19 ± 1.52	1.000	0.234	0.758	0.482	0.918	0.244
	7W	1.27 ± 0.47	1.97 ± 0.74	1.96 ± 2.29	2.19 ± 1.08	0.057	0.619	0.054	0.291	0.954	0.203
	14W	1.52 ± 1.21	1.95 ± 0.99	1.47 ± 1.20	3.36 ± 3.55	0.137	1.000	0.081	0.085	0.573	0.077
HDL-C (mmol/L)	0W	1.60 ± 0.78	1.35 ± 0.46	1.54 ± 0.37	1.27 ± 0.30	0.457	0.452	0.369	0.216	0.898	0.094
	7W	1.50 ± 0.44	1.55 ± 0.46	1.67 ± 0.41	1.43 ± 0.28	0.916	0.241	0.810	0.375	0.817	0.189
	14W	1.50 ± 0.42	1.26 ± 0.34	1.60 ± 0.37	1.31 ± 0.28	0.080	0.452	0.329	0.018	0.411	0.049
LDL-C (mmol/L)	0W	3.20 ± 1.49	3.16 ± 1.12	3.16 ± 1.15	2.90 ± 0.57	0.898	0.560	0.758	0.942	0.608	0.627
	7W	2.98 ± 0.81	3.46 ± 0.93	3.42 ± 1.18	3.23 ± 0.77	0.458	0.126	0.665	0.704	0.452	0.728
	14W	2.76 ± 1.01	2.94 ± 1.03	3.13 ± 1.05	2.67 ± 0.66	0.857	0.286	1.000	0.544	0.488	0.145
Mean glucose (mmol/L)	0W	8.86 ± 2.60	8.25 ± 1.43	7.44 ± 1.35	8.58 ± 2.99	0.862	0.265	0.564	0.147	0.954	0.483
	7W	7.01 ± 0.85	7.89 ± 1.50	7.44 ± 1.07	8.08 ± 1.64	0.378	0.551	0.284	0.625	0.943	0.661
	14W	7.35 ± 1.22	7.13 ± 1.15	7.00 ± 1.07	7.64 ± 1.52	1.000	0.642	0.772	0.704	0.603	0.375
Maximum glucose (mmol/L)	0W	13.5 ± 4.02	12.1 ± 2.00	10.7 ± 1.96	12.6 ± 3.92	0.772	0.076	0.599	0.135	0.862	0.265
	7W	10.6 ± 1.74	11.3 ± 2.04	10.6 ± 1.93	11.6 ± 2.59	0.630	0.914	0.617	0.587	0.721	0.464
	14W	11.9 ± 2.96	10.9 ± 1.20	10.4 ± 2.54	11.1 ± 2.47	0.654	0.375	0.603	0.612	1.000	0.396

Values are presented as mean ± SD unless otherwise indicated. Measurements are shown at baseline (0W), week 7 (7W) and week 14 (14W).

Pairwise P values compare groups at the same time point. Control denotes the non-exercise T2DM control group; LD, LM and LI denote the lactate-decreased, lactate-maintained and lactate-increased exercise-response groups, respectively.

Standard-day CGM variables were calculated after excluding early and late unstable valid days where possible and summarizing retained stable days using 15-min median glucose profiles.

Dietary intake sample sizes varied by group and time point; values with zero SD reflect limited available observations.

Characteristic	Time	Control	LD	LM	LI	Control vs LD	Control vs LM	Control vs LI	LD vs LM	LD vs LI	LM vs LI
Minimum glucose (mmol/L)	0W	5.97 ± 1.62	6.06 ± 1.38	5.58 ± 1.12	6.34 ± 1.97	1.000	0.591	0.916	0.441	0.954	0.563
	7W	4.58 ± 0.88	5.92 ± 1.27	5.50 ± 0.89	6.26 ± 0.91	0.128	0.115	0.018	0.624	0.353	0.130
	14W	5.04 ± 0.93	5.02 ± 0.96	4.87 ± 0.63	5.36 ± 0.86	0.898	0.966	0.685	0.525	0.685	0.217
Glucose excursion (mmol/L)	0W	7.49 ± 2.92	6.07 ± 1.83	5.10 ± 1.39	6.22 ± 2.18	0.354	0.063	0.431	0.364	0.772	0.148
	7W	6.07 ± 2.00	5.36 ± 1.66	5.15 ± 1.59	5.32 ± 2.03	0.575	0.303	0.520	0.957	1.000	1.000
	14W	6.84 ± 2.82	5.86 ± 0.98	5.57 ± 2.42	5.78 ± 1.91	0.749	0.271	0.562	0.582	0.562	0.671
Coefficient of variation (%)	0W	24.2 ± 7.89	19.8 ± 7.17	17.9 ± 4.92	17.5 ± 3.99	0.272	0.076	0.052	0.786	0.452	0.773
	7W	24.6 ± 9.20	17.3 ± 4.10	17.2 ± 4.75	15.9 ± 5.22	0.128	0.116	0.054	0.871	0.830	0.807
	14W	22.9 ± 6.59	22.2 ± 5.50	19.3 ± 6.23	18.5 ± 5.70	0.701	0.254	0.148	0.291	0.148	0.908
TAR (%)	0W	27.3 ± 26.3	22.3 ± 25.8	9.94 ± 14.0	30.3 ± 39.8	0.862	0.127	0.874	0.099	1.000	0.253
	7W	9.90 ± 14.4	16.5 ± 21.6	8.65 ± 13.6	20.4 ± 22.5	0.807	0.692	0.607	0.428	1.000	0.354
	14W	11.2 ± 14.4	7.14 ± 9.19	7.20 ± 11.9	14.7 ± 20.4	1.000	0.404	0.907	0.409	0.861	0.264
TIR (%)	0W	71.2 ± 26.9	77.7 ± 25.8	90.1 ± 14.0	69.7 ± 39.8	0.772	0.107	0.791	0.099	1.000	0.253
	7W	88.2 ± 18.0	83.5 ± 21.6	91.4 ± 13.6	79.6 ± 22.5	0.936	0.435	1.000	0.428	1.000	0.354
	14W	88.2 ± 14.0	89.9 ± 10.2	92.8 ± 11.9	85.3 ± 20.4	0.949	0.334	0.953	0.241	0.907	0.264
VO_{2peak} (mL/kg/min)	0W	24.46 ± 7.37	22.36 ± 3.04	22.36 ± 3.04	25.34 ± 6.14	0.675	0.798	0.866	0.680	0.259	0.428
	14W	26.25 ± 4.61	27.18 ± 6.39	27.92 ± 8.35	28.85 ± 6.33	0.811	0.663	0.511	0.841	0.658	0.800
Rowing resistance level	0W	7.33 ± 2.31	8.57 ± 3.15	7.17 ± 3.27	9.50 ± 2.67	0.518	0.923	0.252	0.372	0.553	0.098

Values are presented as mean ± SD unless otherwise indicated. Measurements are shown at baseline (0W), week 7 (7W) and week 14 (14W).

Pairwise P values compare groups at the same time point. Control denotes the non-exercise T2DM control group; LD, LM and LI denote the lactate-decreased, lactate-maintained and lactate-increased exercise-response groups, respectively.

Standard-day CGM variables were calculated after excluding early and late unstable valid days where possible and summarizing retained stable days using 15-min median glucose profiles.

Dietary intake sample sizes varied by group and time point; values with zero SD reflect limited available observations.

Characteristic	Time	Control	LD	LM	LI	Control vs LD	Control vs LM	Control vs LI	LD vs LM	LD vs LI	LM vs LI
	7W		11.14 ± 2.41	10.27 ± 2.10	11.38 ± 1.69				0.449	0.853	0.223
	14W	8.33 ± 2.08	11.33 ± 3.14	10.55 ± 2.88	12.33 ± 1.03	0.138	0.203	0.066	0.622	0.486	0.085
Total energy intake (kcal/day)	0W	830 ± 284	1061 ± 742	1060 ± 415	770 ± 221	0.874	0.121	0.772	0.767	0.685	0.114
	14W	839 ± 258	815 ± 262	989 ± 447	987 ± 584	0.906	0.724	0.579	0.699	0.773	1.000
Total protein intake (g/day)	0W	39.3 ± 13.5	56.3 ± 47.3	45.1 ± 25.1	39.7 ± 15.8	0.579	0.568	0.913	0.767	0.524	0.671
	14W	36.8 ± 14.2	42.2 ± 10.9	38.5 ± 8.06	41.0 ± 25.8	0.556	0.724	0.460	0.699	0.773	0.773
Total fat intake (g/day)	0W	33.8 ± 16.4	43.7 ± 30.6	41.3 ± 24.1	21.1 ± 7.75	0.526	0.514	0.089	0.899	0.093	0.045
	14W	28.8 ± 14.7	30.9 ± 14.5	63.0 ± 26.7	34.9 ± 29.8	1.000	0.126	0.712	0.245	0.773	0.386
Total carbohydrate intake (g/day)	0W	97.0 ± 39.8	111 ± 75.3	134 ± 43.9	111 ± 46.0	1.000	0.024	0.405	0.473	1.000	0.335
	14W	109 ± 40.6	96.1 ± 20.8	71.8 ± 44.6	133 ± 56.6	0.724	0.195	0.355	0.699	0.773	0.386
Grains and tubers (g/day)	0W	253 ± 116	286 ± 106	425 ± 181	288 ± 117	0.332	0.017	0.585	0.099	0.908	0.097
	14W	283 ± 199	150 ± 0.00	350 ± 129	276 ± 101	0.237	0.358	0.673	0.100	0.139	0.596
Beans and soy products (g/day)	0W	48.6 ± 50.5	30.7 ± 46.3	72.9 ± 101	45.8 ± 41.7	0.146	0.918	0.973	0.139	0.385	0.671
	14W	56.5 ± 61.7	35.4 ± 48.0	48.8 ± 30.4	67.1 ± 11.7	0.747	1.000	0.310	0.817	0.773	0.596
Vegetables (g/day)	0W	247 ± 178	291 ± 330	398 ± 448	244 ± 168	0.851	0.717	0.973	0.702	0.953	0.756
	14W	229 ± 185	450 ± 70.7	412 ± 62.9	267 ± 189	0.193	0.134	0.865	0.617	0.236	0.266
Mushrooms and algae (g/day)	0W	19.0 ± 36.0	36.8 ± 32.5	49.8 ± 62.4	23.2 ± 25.2	0.167	0.029	0.289	0.966	0.524	0.335
	14W	21.0 ± 26.0	23.1 ± 12.5	23.9 ± 15.1	22.9 ± 11.2	0.519	0.525	0.397	0.817	0.773	1.000

Values are presented as mean ± SD unless otherwise indicated. Measurements are shown at baseline (0W), week 7 (7W) and week 14 (14W).

Pairwise P values compare groups at the same time point. Control denotes the non-exercise T2DM control group; LD, LM and LI denote the lactate-decreased, lactate-maintained and lactate-increased exercise-response groups, respectively.

Standard-day CGM variables were calculated after excluding early and late unstable valid days where possible and summarizing retained stable days using 15-min median glucose profiles.

Dietary intake sample sizes varied by group and time point; values with zero SD reflect limited available observations.

Characteristic	Time	Control	LD	LM	LI	Control vs LD	Control vs LM	Control vs LI	LD vs LM	LD vs LI	LM vs LI
Fruits (g/day)	0W	81.2 ± 73.1	102 ± 79.7	136 ± 106	154 ± 104	0.410	0.265	0.080	0.497	0.383	0.755
	14W	131 ± 176	125 ± 106	238 ± 170	164 ± 204	0.746	0.321	0.933	0.487	1.000	1.000
Poultry (g/day)	0W	16.7 ± 25.8	23.2 ± 35.3	15.7 ± 26.9	9.35 ± 4.36	0.970	1.000	0.918	0.832	0.906	0.846
	14W	9.30 ± 15.0	12.5 ± 2.53	7.14 ± 5.83	13.1 ± 2.06	0.195	0.775	0.105	0.340	1.000	0.195
Red meat and offal (g/day)	0W	31.9 ± 34.4	34.2 ± 52.7	41.7 ± 41.3	13.3 ± 9.20	0.709	0.471	0.305	0.374	0.685	0.075
	14W	63.4 ± 66.6	35.7 ± 20.2	87.6 ± 75.0	79.0 ± 105	0.830	0.356	0.800	0.219	1.000	0.471
Dairy products (g/day)	0W	136 ± 118	175 ± 139	159 ± 135	165 ± 145	0.600	0.738	0.609	0.799	0.862	0.847
	14W	130 ± 158	200 ± 0.00	139 ± 104	138 ± 45.4	0.236	0.831	0.446	0.481	0.128	1.000
Eggs (g/day)	0W	31.1 ± 19.4	32.8 ± 24.3	44.6 ± 19.6	33.5 ± 16.5	0.970	0.113	0.888	0.435	1.000	0.210
	14W	34.6 ± 21.2	50.0 ± 0.00	37.5 ± 25.0	47.6 ± 4.12	0.443	0.885	0.440	0.724	0.683	1.000
Fish and aquatic products (g/day)	0W	16.1 ± 16.8	27.9 ± 28.3	41.5 ± 77.7	40.0 ± 66.2	0.455	0.187	0.412	0.899	0.954	0.642
	14W	17.2 ± 17.4	26.8 ± 22.7	13.8 ± 19.7	50.0 ± 12.4	0.590	0.522	0.034	0.348	0.333	0.099
Others (g/day)	0W	44.4 ± 39.2	158 ± 130	98.5 ± 108	37.1 ± 35.8	0.044	0.157	0.562	0.310	0.049	0.153
	14W	79.9 ± 94.8	52.4 ± 57.2	66.2 ± 96.8	82.4 ± 70.0	0.914	0.436	0.554	1.000	0.773	0.860

Values are presented as mean ± SD unless otherwise indicated. Measurements are shown at baseline (0W), week 7 (7W) and week 14 (14W).

Pairwise P values compare groups at the same time point. Control denotes the non-exercise T2DM control group; LD, LM and LI denote the lactate-decreased, lactate-maintained and lactate-increased exercise-response groups, respectively.

Standard-day CGM variables were calculated after excluding early and late unstable valid days where possible and summarizing retained stable days using 15-min median glucose profiles.

Dietary intake sample sizes varied by group and time point; values with zero SD reflect limited available observations.

Fasting lactate showed marked inter-individual heterogeneity rather than a uniform training response (Fig. 3A, B; Table 2). Over 0–14 weeks, fasting lactate decreased in the LD group (− 1.08 ± 1.20 mmol/L), remained relatively stable in the LM group (+ 0.09 ± 0.21 mmol/L) and increased in the LI group (+ 1.15 ± 0.60 mmol/L), whereas the non-exercise control group showed minimal change (− 0.04 ± 0.79 mmol/L). The 0–14-week lactate change differed markedly between LD and LI ($P < 0.001$; Fig. 3B).

Among exercised participants, baseline fasting lactate was inversely associated with the subsequent 0–14-week lactate change ($\rho = -0.63$, $P < 0.001$), indicating that participants with higher baseline lactate tended to show greater reductions after training (Fig. 3C). This pattern was also reflected in the group trajectories: the LD group had the highest fasting lactate at

baseline, whereas the LI group had the highest fasting lactate at week 14. These timepoint-specific comparisons were interpreted descriptively, because the lactate-response groups were defined according to the 0–14-week change in fasting lactate rather than baseline or week-14 lactate values alone (Table 2).

Despite divergent lactate trajectories, conventional glycaemic markers changed similarly across groups. HbA1c decreased across all three exercise groups, with no significant group-by-time effect (P = 0.931, q = 0.931; Table 2). Fasting glucose also showed no significant group-specific interaction (P = 0.854, q = 0.854; Fig. 3C; Fig. S2A).

To further examine whether lactate-response heterogeneity simply reflected changes in fasting glucose, we regrouped intervention participants into glucose-decreased, glucose-maintained and glucose-increased tertiles according to the 0–14-week change in fasting glucose. These glucose-change categories did not correspond one-to-one with the lactate-response groups (Fig. S2C). Baseline fasting glucose was not significantly associated with baseline fasting lactate (Spearman ρ = 0.24, P = 0.141), and the 0–14-week changes in fasting glucose and fasting lactate were also not significantly correlated (Spearman ρ = 0.19, P = 0.232; Fig. S2E, F). These findings suggest that fasting lactate-response heterogeneity was not simply explained by fasting glucose changes.

In contrast, insulin-related and lipid markers showed a more adverse response pattern in the LI group. Fasting insulin remained broadly unchanged in LD, decreased slightly in LM and increased in LI (+ 59.5% vs. control; group-by-time P = 0.017, q = 0.096; Fig. 3C; Table 2). A similar pattern was observed for HOMA-IR, which decreased in LD, remained relatively stable in LM and increased in LI (+ 76.4% vs. control; P = 0.031, q = 0.132; Fig. 3C; Table 2). Triglycerides showed the clearest group-specific lipid response, increasing in LI (+ 87.6% vs. control), with a significant group-by-time effect after FDR correction (P = 0.004, q = 0.021; Fig. S2A, B; Table 2). At week 14, fasting insulin, HOMA-IR and triglycerides were numerically highest in LI, supporting a more adverse insulin–lipid profile in this group. However, week-14 pairwise contrasts among LD, LM and LI were interpreted cautiously because the lactate-response groups were defined according to 0–14-week lactate change (Table 2).

Standard-day continuous glucose monitoring profiles improved broadly across groups but did not explain the divergent lactate responses (Fig. 3D, E; Table 2). Mean glucose decreased, time above range decreased and time in range increased in all three exercise groups, with no significant group-by-time interactions. Week-14 pairwise comparisons showed no significant differences among LD, LM and LI for mean glucose, TAR or TIR, indicating broadly comparable CGM-derived glycaemic profiles despite divergent lactate responses (Table 2).

Exercise capacity showed an overall improvement across trained groups, as reflected by increased VO_{2peak} and rowing resistance level from baseline to week 14 in LD, LM and LI, with no significant week-14 pairwise differences among the exercise response groups (Table 2). Dietary intake was assessed at baseline and week 14. At week 14, total energy and macronutrient intake were comparable across groups, and nominal differences in selected food categories did not show a consistent pattern aligned with lactate-response groups. Therefore, dietary intake was interpreted as descriptive contextual information rather than a primary explanation for the divergent lactate responses (Table 2).

Together, these findings indicate that 14 weeks of HIIT induced heterogeneous fasting lactate responses in patients with T2DM. Although glycaemic control and exercise capacity improved broadly across the trained groups, the LI group was accompanied by more adverse insulin-resistance and triglyceride response patterns. The glucose-change regrouping analyses further suggested that fasting lactate response and fasting glucose change represented partially distinct clinical axes. These results support the interpretation that fasting lactate response captures a distinct dimension of metabolic adaptation beyond conventional glucose improvement.

Divergent fasting lactate responses are accompanied by lipid- and redox-related serum metabolomic remodelling

To explore metabolomic features associated with divergent lactate adaptation, we examined selected serum metabolite features across lactate-response groups during the 14-week HIIT intervention. Timepoint-wise LD–LI comparisons showed

exploratory metabolite differences at baseline, week 7 and week 14, involving indole-related metabolites, acylcarnitines, fatty-acid-related metabolites and amino acid-related metabolites (Fig. 4A). Labelled examples included 5-hydroxytryptophol, indoleacetyl glutamine, arachidyl carnitine and hexacosanoyl carnitine at baseline; S-japonin, 1H-indole-3-carboxaldehyde, 3-oxooctadecanoic acid and veranisatin C at week 7; and 2-hydroxybutyric acid, 13S-hydroxyoctadecadienoic acid, citrulline and (2R)-O-phospho-3-sulfolactate at week 14. These comparisons were interpreted as exploratory LD–LI contrasts rather than definitive metabolite-discovery findings.

We then focused on metabolite features whose 0–14-week changes were associated with week-14 fasting lactate after adjustment for baseline fasting lactate and age. Among the ranked candidates, PI(17:0/14:1(9Z)) showed the strongest adjusted association with week-14 lactate (β = 0.369, P = 1.42 × 10^-5, FDR = 0.032, incremental R^2 = 0.46; Fig. 4B, D, E; Table S1). Other top-ranked features included PG(14:0/0:0) (β = −0.343, P = 9.72 × 10^-5, FDR = 0.109, incremental R^2 = 0.40), PC(14:1(9Z)/22:2(13Z,16Z)) (β = 0.329, P = 2.15 × 10^-4, FDR = 0.161, incremental R^2 = 0.37) and ubiquinone Q1 (β = 0.328, P = 6.77 × 10^-4, FDR = 0.253, incremental R^2 = 0.32; Fig. 4B, D; Table S1). Adjusted feature–lactate fits were shown for PI(17:0/14:1(9Z)) and PG(14:0/0:0) as representative phospholipid candidates (Fig. 4E).

The signed incremental R^2 summary further identified additional response-associated candidates, including galactosylglycerol, sphinganine 1-phosphate, cis-5-tetradecenoylcarnitine, 8Z-heptadecene, isovalerylcarnitine and sphingosine 1-phosphate (P = 0.00250–0.00684; FDR = 0.362–0.388; incremental R^2 = 0.224–0.270; Fig. 4D; Table S1). Together, these ranked features suggest that longitudinal lactate adaptation was mainly associated with phospholipid-, sphingolipid-, acylcarnitine/fatty-acid- and redox-related metabolite features.

Group-time analysis further supported these metabolite classes, highlighting sphingolipid, acylcarnitine, fatty-acid/dicarboxylate, glycerophospholipid and redox-related features, including sphinganine 1-phosphate, sphingosine 1-phosphate, isovalerylcarnitine, oleoylcarnitine, 8E-heptadecenedioic acid, PI(17:0/14:1(9Z)), PG(14:0/0:0), PC(14:1(9Z)/22:2(13Z,16Z)) and ubiquinone Q1 (Fig. 4C; Table S1). The metabolite module network organized selected lactate-associated candidates around lactate into membrane phospholipid remodelling, fatty-acyl/carnitine energy handling, sphingolipid signalling and redox-carbon metabolism modules (Fig. 4F). This network was used as an exploratory visualization of selected candidates rather than evidence of causal molecular interactions.

Supplementary analyses showed that age differed across groups (P = 0.016), whereas BMI, sex distribution and drug-class count did not differ significantly (P = 0.629, P = 0.449 and P = 0.760, respectively; Fig. S3A; Table S3). Accordingly, age was included as an adjustment covariate in the feature–lactate association models. The supplementary heatmap displayed additional lactate-associated features across control, LD, LM and LI groups, including phospholipid-, sphingolipid-, acylcarnitine- and glycolipid-related metabolites (Fig. S3B). Overall, these exploratory metabolomic results indicate that divergent fasting lactate responses after HIIT were associated with phospholipid remodelling, sphingolipid signalling, acylcarnitine/fatty-acid handling and redox-related metabolic features, rather than isolated changes in lactate concentration alone.

Divergent fasting lactate responses are accompanied by systemic serum proteomic remodelling

To further examine whether divergent lactate adaptation was accompanied by serum proteomic remodelling, we profiled selected protein features across lactate-response groups during the 14-week HIIT intervention. Timepoint-wise LD–LI comparisons showed exploratory protein differences at baseline, week 7 and week 14 (Fig. 5A). Labelled features included COG4, PIM3, METAP2 and IGHV5-10-1 at baseline; GHRL, ADGRF5, ATM and CAPRIN2 at week 7; and TGFB1, ANGPTL6, TSTD1 and SNX12 at week 14. These comparisons were interpreted as exploratory LD–LI contrasts rather than definitive protein-discovery findings.

We then focused on protein features whose 0–14-week changes were associated with week-14 fasting lactate after adjustment for baseline fasting lactate, age, sex, BMI and drug-class count. Representative protein features included DRG1 (β

= −0.579, P = 8.27 × 10^-4, incremental R² = 0.379), CRYBG3 (β = 0.337, P = 0.0014, incremental R² = 0.425), FCN2 (β = 0.363, P = 0.0030, incremental R² = 0.375) and NOTUM (β = 0.331, P = 0.0027, incremental R² = 0.297; Fig. 5B, D; Table S2). DRG1 was negatively associated with week-14 lactate, whereas CRYBG3, FCN2 and NOTUM were positively associated. Adjusted protein–lactate fits were shown for DRG1 and NOTUM as representative examples (Fig. 5E). Because these candidates did not survive feature-level FDR correction, they were interpreted as exploratory protein features associated with lactate-response patterns.

The signed incremental R² summary further identified additional response-associated proteins, including ANKRD26, PPP2R2C, ANGPTL8, CIDEB, TP53RK and CES1 (P = 0.00523–0.0104; incremental R² = 0.214–0.488; Fig. 5D; Table S2). Group-time protein abundance analysis supported this pattern, highlighting features with endpoint/group and timepoint evidence, including FGA, FGG, ANGPTL2, RGPD1, CES1, NUCB1, ANKRD26, NOTUM, CRYBG3 and DRG1 (Fig. 5C; Table S2).

Functional module mapping organized selected lactate-associated proteins into lipid/adipokine remodelling, immune/complement activity, extracellular remodelling and cellular stress/RNA regulation modules (Fig. 5F). The module network included DRG1, PPP2R2C, TP53RK and EIF4ENIF1 within the cellular stress/RNA regulation module; FCN2 and SERPINA6 within the immune/complement module; NOTUM within the extracellular remodelling module; and ANGPTL8, CIDEB and CES1 within the lipid/adipokine remodelling module. This network was used as an exploratory visualization of selected candidates rather than evidence of causal protein interactions.

The supplementary heatmap further displayed additional lactate-associated protein features across the control, LD, LM and LI groups, including ANKRD26, PPP2R2C, ANGPTL8, CIDEB, TP53RK, CES1, SERPINA6, EIF4ENIF1, TGM2, DNAJB11, UTY and CCL17 (Fig. S4). Together, these exploratory proteomic results indicate that divergent fasting lactate responses after HIIT were accompanied by serum protein remodelling related to lipid/adipokine signalling, immune/complement activity, extracellular remodelling and cellular stress/RNA regulation.

Integrated lactate-centred multi-omics network summarizes time-layered clinical and molecular features of lactate-response heterogeneity

To integrate the clinical, metabolomic and proteomic findings, we constructed an exploratory lactate-centred network linking selected features associated with baseline fasting lactate, adjusted 0–14-week lactate response and week-14 fasting lactate (Fig. 6). After figure-level pruning, the final displayed network retained 119 nodes and 189 edges, including 21 baseline nodes, 65 response-layer nodes and 33 week-14 nodes. The response layer formed the densest component, consistent with the primary analytical focus on continuous lactate-response heterogeneity.

The clinical layer connected the lactate-related time layers with selected insulin- and lipid-related indices. At baseline, fasting lactate was positively associated with HOMA-IR (β = 0.536, P = 0.004, FDR = 0.050, incremental R² = 0.203), HbA1c (β = 0.410, P = 0.021, FDR = 0.107, incremental R² = 0.138) and fasting insulin (β = 0.403, P = 0.027, FDR = 0.107, incremental R² = 0.128). At week 14, fasting lactate was positively associated with triglycerides (β = 0.547, P = 3.12 × 10^-4, FDR = 0.004, incremental R² = 0.226) and negatively associated with age (β = −0.495, P = 0.001, FDR = 0.007, incremental R² = 0.245). In the response layer, triglyceride change was positively associated with adjusted lactate response (β = 0.474, P = 0.002, FDR = 0.024, incremental R² = 0.225), supporting a clinical link between lactate-response heterogeneity and insulin–lipid metabolic context.

The metabolomic layer organized selected candidate features into glycerophospholipid remodelling, fatty-acyl/carnitine handling, sphingolipid signalling, redox-carbon metabolism and carbon/carbohydrate-related context. In the response layer, representative lactate-associated metabolite features included PI(17:0/14:1) (β = 0.369, P = 1.42 × 10^-5, FDR = 0.032, incremental R² = 0.458), PG(14:0/0:0) (β = −0.343, P = 9.72 × 10^-5, FDR = 0.109, incremental R² = 0.396), PC(14:1/22:2) (β = 0.329, P = 2.15 × 10^-4, FDR = 0.161, incremental R² = 0.368), ubiquinone Q1 (β = 0.328, P = 6.77 × 10^-4, FDR = 0.253,

incremental R^2 = 0.324) and sphinganine 1-phosphate (β = −0.310, P = 0.003, FDR = 0.362, incremental R^2 = 0.259). Week-14 metabolite associations provided additional endpoint context, including the redox-related feature 2-chloro-1,4-naphthoquinone (β = −0.499, P = 2.14 × 10^-4, FDR = 0.080, incremental R^2 = 0.404).

The proteomic layer organized candidate serum proteins into cellular stress/RNA regulation, immune/complement activity, extracellular remodelling and lipid/adipokine modules. Response-layer protein features included DRG1 (β = −0.579, P = 8.27 × 10^-4, FDR = 0.991, incremental R^2 = 0.379), FCN2 (β = 0.363, P = 0.003, FDR = 0.991, incremental R^2 = 0.375), NOTUM (β = 0.331, P = 0.003, FDR = 0.991, incremental R^2 = 0.297), PPP2R2C (β = 0.336, P = 0.006, FDR = 0.991, incremental R^2 = 0.276), ANGPTL8 (β = 0.293, P = 0.009, FDR = 0.991, incremental R^2 = 0.237), CIDEB (β = 0.257, P = 0.010, FDR = 0.991, incremental R^2 = 0.219) and CES1 (β = 0.331, P = 0.010, FDR = 0.991, incremental R^2 = 0.263). Week-14 protein features, including TGFB1, ANGPTL6, SPP2 and OIT3, provided additional endpoint context for extracellular and lipid/adipokine-related remodelling.

Across the network, 93 lactate-to-molecular feature edges and 63 module-to-feature edges linked selected proteins and metabolites with lactate-centred time layers and functional modules. The retained modules emphasized glycerophospholipid and sphingolipid remodelling, fatty-acyl/carnitine handling, redox-carbon metabolism, immune/complement activity, extracellular remodelling and lipid/adipokine context. Overall, this integrated network provides a time-layered systems-level summary linking baseline lactate state, insulin–lipid clinical context, metabolomic remodelling and circulating protein features. Because the network was pathway-guided and exploratory, it should be interpreted as a hypothesis-generating framework rather than evidence of causal mediation, independent prediction or a validated biomarker panel.

Exploratory lactate-centred network summarizing clinical, metabolomic and proteomic associations around fasting lactate at baseline, adjusted lactate response over 0–14 weeks and post-intervention fasting lactate at week 14. The three shaded regions indicate baseline, lactate-response and post-intervention layers. Central lactate nodes are connected along the temporal lactate axis. Node shape denotes data class: triangles, clinical indices; diamonds, metabolites; circles, proteins; and large pale circles, functional modules. Node colour indicates the direction of association where available, with red representing positive beta coefficients and blue representing negative beta coefficients. Node border indicates statistical support, including FDR < 0.10 or nominal evidence. Pale gold halos indicate features traceable to Fig. 3–5 evidence. Edges indicate lactate associations, lactate–molecule links, module–feature membership, repeated features across time layers or prior pathway support. The network is pathway-guided and hypothesis-generating and should not be interpreted as evidence of causal mediation or validated mechanisms.

BMI, body mass index; FDR, false discovery rate; HbA1c, glycated haemoglobin; HIIT, high-intensity interval training; HOMA-IR, homeostasis model assessment of insulin resistance; TG, triglycerides.

Discussion

In this study, we identified fasting lactate response as a heterogeneous metabolic adaptation phenotype in patients with T2DM undergoing 14 weeks of supervised HIIT. Three major findings emerged. First, patients with T2DM already exhibited higher fasting lactate at baseline, together with impaired glucose-insulin homeostasis and exploratory metabolomic disturbances in lactate-connected metabolic axes despite comparable physical activity and most lipid markers. Second, HIIT induced divergent fasting lactate responses: lactate decreased in LD, remained relatively stable in LM, and increased in LI, despite improved glucose control and exercise capacity across groups. Third, the LI group was accompanied by increased insulin resistance and triglycerides, together with exploratory metabolomic and proteomic features related to phospholipid and sphingolipid remodelling, acylcarnitine/fatty-acid handling, redox-related metabolism, and systemic lipid-adipokine, immune/complement and extracellular remodelling.

The baseline elevation of fasting lactate in T2DM supports the concept that lactate is not simply an anaerobic waste product but an active intermediate in systemic carbon trafficking, mitochondrial oxidation, gluconeogenesis, and metabolic signalling[9, 10]. Contemporary lactate shuttle theory emphasizes that lactate is continuously produced and consumed under aerobic conditions, functioning as an energy substrate and signalling molecule across organs[9, 10]. Recent human tracer data further show that lactate is a major vehicle for dietary carbohydrate carbon distribution, reinforcing its central role in systemic

substrate flux[12]. In this context, the higher fasting lactate observed in T2DM may reflect altered coupling between glycolytic carbon flow, pyruvate oxidation, hepatic glucose handling, and peripheral substrate utilization rather than isolated lactate overproduction. This baseline difference may also be influenced by medication use, including metformin[26]. As exercise intervention and metformin are both central to T2DM management, this provides a clinically relevant context for evaluating lactate adaptation after exercise training.

Our longitudinal findings extend previous exercise studies in T2DM by showing that basal lactate adaptation is highly heterogeneous. Previous meta-analytic evidence suggested that chronic exercise training may improve lactate responses during exercise, but has inconsistent effects on resting lactate concentrations in T2DM[27]. Similarly, HIIT is generally reported to improve glycaemic control, cardiorespiratory fitness, and lipid metabolism in T2DM[28]. Consistent with this, our participants showed broad improvements in glycaemic control, CGM profiles, and exercise capacity. However, these conventional benefits did not fully explain the divergent fasting lactate trajectories. This dissociation suggests that fasting lactate response may capture a distinct layer of metabolic adaptation beyond HbA1c, fasting glucose, or CGM-derived glucose exposure.

A key observation was that the LI group showed unfavorable insulin and triglyceride trajectories, despite preserved training adaptation on glycaemic control. This pattern is clinically relevant because insulin resistance and dyslipidemia are central components of cardiometabolic risk in T2DM. Metabolomics studies have consistently shown that amino acids, lipids, carbohydrates, acylcarnitines, and related substrate-handling metabolites are associated with T2DM risk and insulin resistance[15, 16, 29]. In particular, altered BCAA metabolism and acylcarnitine profiles have been linked to impaired insulin action and incomplete substrate oxidation[15, 29]. Our baseline and intervention metabolomic findings are aligned with this literature, but add a lactate-centered perspective: the difference between LD and LI was not limited to lactate itself, but involved multiple metabolic axes connected to lactate production, oxidation, and competing substrate flux.

The intervention metabolomic results provided an exploratory molecular context for these divergent lactate responses. In the adjusted endpoint models, several metabolites feature whose 0–14-week changes were associated with 14-week fasting lactate mapped primarily to glycerophospholipid, sphingolipid, acylcarnitine, fatty-acid/dicarboxylate and redox-related modules. PI(17:0/14:1(9Z)) showed the strongest adjusted association with 14-week lactate, whereas PG(14:0/0:0), PC(14:1(9Z)/22:2(13Z,16Z)) and ubiquinone Q1 were additional top-ranked features. These findings suggest that lactate-response heterogeneity was accompanied by changes in membrane lipid remodelling, lipid-associated substrate handling and redox-related metabolism, rather than isolated changes in lactate concentration alone. Because these analyses were exploratory and based on untargeted LC-MS annotations, individual metabolite identities and pathway interpretations should be considered hypothesis-generating.

The directional metabolomic contrasts at week 14 further supported this interpretation. Features higher in LD included 2-hydroxybutyric acid, 13S-hydroxyoctadecadienoic acid and 3-oxohexadecanoic acid, whereas features higher in LI included citrulline, ornithine and (2R)-O-phospho-3-sulfolactate. Although these differences were nominal and should not be interpreted as definitive pathway-level changes, they are consistent with the possibility that lactate adaptation is linked to differences in oxidative stress-related, amino acid/nitrogen-related and lipid oxidation-associated substrate handling. This pattern also aligns with the clinical observation that the LI group showed both increased fasting lactate and a more adverse triglyceride trajectory after HIIT. Thus, increased fasting lactate may not simply indicate a failure of glucose lowering, but may instead reflect persistent or emerging substrate-handling stress, particularly involving lipid-related fuel use or metabolic flexibility.

The proteomic results further supported a systemic remodelling interpretation. In the adjusted endpoint models, CRYBG3, DRG1, FCN2 and NOTUM were representative protein features whose 0–14-week changes were associated with 14-week fasting lactate. These proteins do not represent canonical lactate-metabolism enzymes but instead point to systemic biological processes, including immune/complement activity, extracellular signalling and cellular stress-related regulation. At 14 weeks, LI showed higher abundance of TGFB1, ANGPTL6, SPP2, OIT3 and SNED1, whereas LD showed higher abundance

of TSTD1, SNX12, GHRL and ABI1. Supplementary protein features, including ANGPTL8, CIDEB, CES1, SERPINA6, TGM2 and CCL17, further suggested lipid-adipokine, immune/inflammatory, extracellular remodelling and systemic protein signatures. ANGPTL6 has been linked to clinical metabolic features in patients with T2DM, and complement-related proteins may contribute to inflammatory and cardiometabolic complications of diabetes[30–31]. Therefore, the proteomic data do not indicate direct alteration of canonical lactate enzymes such as LDH, MCT or PDH. Instead, they suggest that the lactate-increased phenotype reflects lipid-systemic and immune-related remodelling.

Taken together, our findings support a model in which fasting lactate response acts as an integrative marker of exercise-induced metabolic adaptation in T2DM. In the lactate decreased group, lactate reduction may be consistent with more favourable coordination between glycolytic carbon flow, oxidative substrate handling, redox adaptation and lipid remodelling. In the lactate increased group, lactate increase may identify individuals in whom exercise improves glucose control and fitness but is accompanied by persistent insulin-lipid stress and systemic lipid-adipokine, immune/complement and extracellular remodelling. This interpretation is consistent with emerging precision metabolomics frameworks, which emphasize that metabolite responses can reveal inter-individual differences in insulin resistance, substrate utilization and cardiometabolic risk beyond standard clinical markers[15].

This study has several limitations. The lactate-response groups were defined by fasting lactate change; therefore, lactate group comparisons should be interpreted as phenotype-defining rather than independent validation of lactate change. The metabolomic and proteomic analyses were exploratory, and most full-feature FDR-corrected results did not reach statistical significance. Metabolite annotations from untargeted LC-MS should be considered putative unless validated by targeted assays. The sample size was modest, and mechanistic tissues such as skeletal muscle, adipose tissue and liver were not directly assessed. In addition, the current serum proteomic findings reflect circulating protein features and do not establish direct tissue-specific mechanisms of lactate transport or oxidation. Future studies should include larger independent cohorts, targeted validation of lactate-associated metabolites and candidate proteins, isotope-tracer approaches to quantify lactate flux, and tissue-level analyses of lactate transport, pyruvate oxidation, mitochondrial function and lipid handling.

Conclusions

Fasting lactate response revealed marked heterogeneity in metabolic adaptation to 14-week HIIT among patients with T2DM. Although glycaemic control and exercise capacity improved overall, participants with increased lactate showed more adverse insulin-resistance and triglyceride response patterns. Exploratory metabolomic and proteomic analyses further linked divergent lactate responses to lipid-associated substrate handling, redox-related metabolism and systemic lipid-immune remodelling. These findings suggest that fasting lactate response may serve as an integrative marker of exercise-induced metabolic adaptation beyond conventional glucose outcomes in T2DM, warranting targeted validation in larger independent cohorts.

Abbreviations

BCAA
branched-chain amino acid
BMI
body mass index
CGM
continuous glucose monitoring
CV
coefficient of variation
DIA
data-independent acquisition
DXA

dual-energy X-ray absorptiometry
FDR
false discovery rate
HbA1c
glycated haemoglobin
HDL-C
high-density lipoprotein cholesterol
HIIT
high-intensity interval training
HMDB
Human Metabolome Database
HOMA-IR
homeostasis model assessment of insulin resistance
ISI
insulin sensitivity index
LC–MS
liquid chromatography–mass spectrometry
LC–MS/MS
liquid chromatography–tandem mass spectrometry
LD
lactate decreased
LDL-C
low-density lipoprotein cholesterol
LI
lactate increased
LM
lactate maintained
OGTT
oral glucose tolerance test
PCA
principal component analysis
QC
quality control
T2DM
type 2 diabetes mellitus
TAR
time above range
TCA
tricarboxylic acid
TIR
time in range
VO_2peak
peak oxygen uptake

Declarations

Declaration of generative AI and AI-assisted technologies in the manuscript preparation process

During the preparation of this manuscript, the authors used ChatGPT to improve language readability and to assist with drafting and refining code for data visualization. All statistical analyses, figure outputs and manuscript content were reviewed, verified and edited by the authors. The authors take full responsibility for the accuracy, integrity and final content of the manuscript.

Ethics approval and consent to participate

This study was approved by the Ethics Committee for Human Studies of Shanghai Jiao Tong University (approval numbers: ML16027 and B2020023I) and was conducted in accordance with the Declaration of Helsinki. All participants provided written informed consent before enrolment.

Consent for publication

Not applicable.

Competing Interests

Professor Jingyan Tian, a co-author of this manuscript, is serving as a Guest Editor for this Collection. We respectfully request that the manuscript be handled independently according to the journal's editorial policy, without her involvement in the editorial assessment or peer-review process.

Funding

This study was supported by the National Natural Science Foundation of China (grant number 82370902), the China Postdoctoral Science Foundation (grant number 2025M783218), and by the project of Shanghai Jiaotong University research and development of exercise intervention strategies and precision exercise prescriptions for type 2 diabetes (18H500000044).

Author Contribution

JG, YW, XW, KQ and SC conceived the study framework. JG and YW performed data curation, generated the figures and drafted the manuscript. HZ, TZ and NC implemented the exercise intervention and contributed to data acquisition and curation. XL, NC, CW, TG, WX and KQ performed the omics and bioinformatics analyses. JT, KC and QL provided medical support during the intervention and contributed to clinical data analysis. WX and LY critically reviewed the manuscript and provided substantial revisions and feedback. XW, KQ and SC contributed to study design, funding acquisition, data interpretation, project supervision and critical revision of the manuscript for important intellectual content. SC was the principal investigator, designed the study, provided overall supervision, reviewed the study process and substantially revised the manuscript through multiple iterations. All authors read and approved the final manuscript.

Acknowledgement

We would like to thank the researchers who contributed to the cross-sectional validation data project, including Prof. Daxian Lu and Drs. Xican Zhao, Jun Ge, Zhengchang Xia, Xiaming Du and Shenglong Le, for their valuable support and contributions. We also thank the undergraduate, graduate and postdoctoral students in Prof. Cheng's group who contributed to data collection and implementation of the exercise intervention throughout this study. We sincerely thank all participants for generously volunteering their time and taking part in the study. In addition, we are grateful to the Instrumental Analysis Center

of Shanghai Jiao Tong University and Shanghai Yisuan Biotechnology Co., Ltd. for their technical assistance and professional support in the measurement and analysis of the metabolomic and proteomic data.

Availability of data and materials

The datasets generated and analysed during the current study are not publicly available due to ethical restrictions surrounding individual-level clinical and omics data. However, they are available from the corresponding author upon reasonable request, subject to institutional and ethical approval.

References

1. Blaha MJ, Khorsandi M. Type 2 diabetes mellitus: now in the cardiologist's wheelhouse. J Am Coll Cardiol. 2023;82(16):1595–7. 10.1016/j.jacc.2023.08.033.
2. Gyldenkerne C, Mortensen MB, Kahlert J, Thrane PG, Warnakula Olesen KK, Sorensen HT, et al. 10-year cardiovascular risk in patients with newly diagnosed type 2 diabetes mellitus. J Am Coll Cardiol. 2023;82(16):1583–94. 10.1016/j.jacc.2023.08.015.
3. Roden M, Shulman GI. The integrative biology of type 2 diabetes. Nature. 2019;576(7785):51–60. 10.1038/s41586-019-1797-8.
4. American Diabetes Association Professional Practice Committee. 5. Facilitating positive health behaviors and well-being to improve health outcomes: Standards of Care in Diabetes—2025. Diabetes Care. 2025;48(Suppl 1):S86–S127. 10.2337/dc25-S005
5. Zhao T, Yang Q, Feuerbacher JF, Yu B, Brinkmann C, Cheng S, et al. Effects of exercise, metformin and their combination on glucose metabolism in individuals with abnormal glycaemic control: a systematic review and network meta-analysis. Br J Sports Med. 2024;58(23):1452–60. 10.1136/bjsports-2024-108127.
6. American Diabetes Association Professional Practice Committee. 9. Pharmacologic approaches to glycemic treatment: Standards of Care in Diabetes—2025. Diabetes Care. 2025;48(Suppl 1):S181–S206. 10.2337/dc25-S009
7. Foretz M, Guigas B, Viollet B. Metformin: update on mechanisms of action and repurposing potential. Nat Rev Endocrinol. 2023;19(8):460–76. 10.1038/s41574-023-00833-4.
8. LaMoia TE, Shulman GI. Cellular and molecular mechanisms of metformin action. Endocr Rev. 2021;42(1):77–96. 10.1210/endrev/bnaa023.
9. Brooks GA, Arevalo JA, Osmond AD, Leija RG, Curl CC, Tovar AP. Lactate in contemporary biology: a phoenix risen. J Physiol. 2022;600(5):1229–51. 10.1113/JP280955.
10. Brooks GA, Osmond AD, Arevalo JA, Duong JJ, Curl CC, Moreno-Santillan DD, et al. Lactate as a myokine and exerkine: drivers and signals of physiology and metabolism. J Appl Physiol. 2023;134(3):529–48. 10.1152/japplphysiol.00497.2022.
11. Li X, Yang Y, Zhang B, Lin X, Fu X, An Y, et al. Lactate metabolism in human health and disease. Signal Transduct Target Ther. 2022;7(1):305. 10.1038/s41392-022-01151-3.
12. Leija RG, Curl CC, Arevalo JA, Osmond AD, Duong JJ, Huie MJ, et al. Enteric and systemic postprandial lactate shuttle phases and dietary carbohydrate carbon flow in humans. Nat Metab. 2024;6(4):670–7. 10.1038/s42255-024-00993-1.
13. Cheng C, Liu Y, Sun L, Fan J, Sun X, Zheng JS, et al. Integrative metabolomics and genomics reveal molecular signatures for type 2 diabetes and its cardiovascular complications. Cardiovasc Diabetol. 2025;24(1):166. 10.1186/s12933-025-02718-4.
14. Morze J, Wittenbecher C, Schwingshackl L, Danielewicz A, Rynkiewicz A, Hu FB, et al. Metabolomics and type 2 diabetes risk: an updated systematic review and meta-analysis of prospective cohort studies. Diabetes Care. 2022;45(4):1013–24. 10.2337/dc21-1705.

15. Rizo-Roca D, Henderson JD, Zierath JR. Metabolomics in cardiometabolic diseases: key biomarkers and therapeutic implications for insulin resistance and diabetes. J Intern Med. 2025;297(6):584–607. 10.1111/joim.20090.
16. Vanweert F, Schrauwen P, Phielix E. Role of branched-chain amino acid metabolism in the pathogenesis of obesity and type 2 diabetes-related metabolic disturbances. Nutr Diabetes. 2022;12(1):35. 10.1038/s41387-022-00213-3.
17. Liu WY, Lu DJ, Du XM, Sun JQ, Ge J, Wang RW, et al. Effect of aerobic exercise and low carbohydrate diet on pre-diabetic non-alcoholic fatty liver disease in postmenopausal women and middle aged men: the role of gut microbiota composition: study protocol for the AELC randomized controlled trial. BMC Public Health. 2014;14(1):48. 10.1186/1471-2458-14-48.
18. Cheng S, Ge J, Zhao C, Le S, Yang Y, Ke D, et al. Effect of aerobic exercise and diet on liver fat in pre-diabetic patients with non-alcoholic-fatty-liver-disease: a randomized controlled trial. Sci Rep. 2017;7(1):15952. 10.1038/s41598-017-16159-x.
19. Cheng R, Wang L, Le S, Yang Y, Zhao C, Zhang X, et al. A randomized controlled trial for response of microbiome network to exercise and diet intervention in patients with nonalcoholic fatty liver disease. Nat Commun. 2022;13(1):2555. 10.1038/s41467-022-29968-0.
20. Cheung YM, Roff G, Grossmann M. Precision of the Hologic Horizon A dual energy X-ray absorptiometry in the assessment of body composition. Obes Res Clin Pract. 2020;14(6):514–8. 10.1016/j.orcp.2020.10.005.
21. American College of Sports Medicine. In: Liguori G, editor. ACSM's Guidelines for Exercise Testing and Prescription. 11 ed. Philadelphia: Wolters Kluwer; 2021.
22. Matthews DR, Hosker JP, Rudenski AS, Naylor BA, Treacher DF, Turner RC. Homeostasis model assessment: insulin resistance and beta-cell function from fasting plasma glucose and insulin concentrations in man. Diabetologia. 1985;28(7):412–9. 10.1007/BF00280883.
23. Matsuda M, DeFronzo RA. Insulin sensitivity indices obtained from oral glucose tolerance testing: comparison with the euglycemic insulin clamp. Diabetes Care. 1999;22(9):1462–70. 10.2337/diacare.22.9.1462.
24. Battelino T, Danne T, Bergenstal RM, Amiel SA, Beck R, Biester T, et al. Clinical targets for continuous glucose monitoring data interpretation: recommendations from the International Consensus on Time in Range. Diabetes Care. 2019;42(8):1593–603. 10.2337/dci19-0028.
25. American Diabetes Association Professional Practice Committee. 7. Diabetes Technology: Standards of Care in Diabetes—2025. Diabetes Care. 2025;48(Suppl 1):S146–S166. 10.2337/dc25-S007
26. Madiraju AK, Erion DM, Rahimi Y, Zhang XM, Braddock DT, Albright RA, et al. Metformin suppresses gluconeogenesis by inhibiting mitochondrial glycerophosphate dehydrogenase. Nature. 2014;510(7506):542–6. 10.1038/nature13270.
27. Zhao T, Le S, Freitag N, Schumann M, Wang X, Cheng S. Effect of chronic exercise training on blood lactate metabolism among patients with type 2 diabetes mellitus: a systematic review and meta-analysis. Front Physiol. 2021;12:652023. 10.3389/fphys.2021.652023.
28. Feng J, Zhang Q, Chen B, Chen J, Wang W, Hu Y, et al. Effects of high-intensity intermittent exercise on glucose and lipid metabolism in type 2 diabetes patients: a systematic review and meta-analysis. Front Endocrinol. 2024;15:1360998. 10.3389/fendo.2024.1360998.
29. Hosseinkhani S, Arjmand B, Dilmaghani-Marand A, Mohammadi Fateh S, Dehghanbanadaki H, Najjar N, et al. Targeted metabolomics analysis of amino acids and acylcarnitines as risk markers for diabetes by LC-MS/MS technique. Sci Rep. 2022;12(1):8418. 10.1038/s41598-022-11970-7.
30. Takebayashi K, Suzuki T, Yamauchi M, Hara K, Tsuchiya T, Inukai T, et al. Circulating angiopoietin-like protein 6 levels and clinical features in patients with type 2 diabetes. Intern Med. 2025;64(5):643–9. 10.2169/internalmedicine.3609-24.
31. Ajjan RA, Schroeder V. Role of complement in diabetes. Mol Immunol. 2019;114:270–7. 10.1016/j.molimm.2019.07.031.

Figures

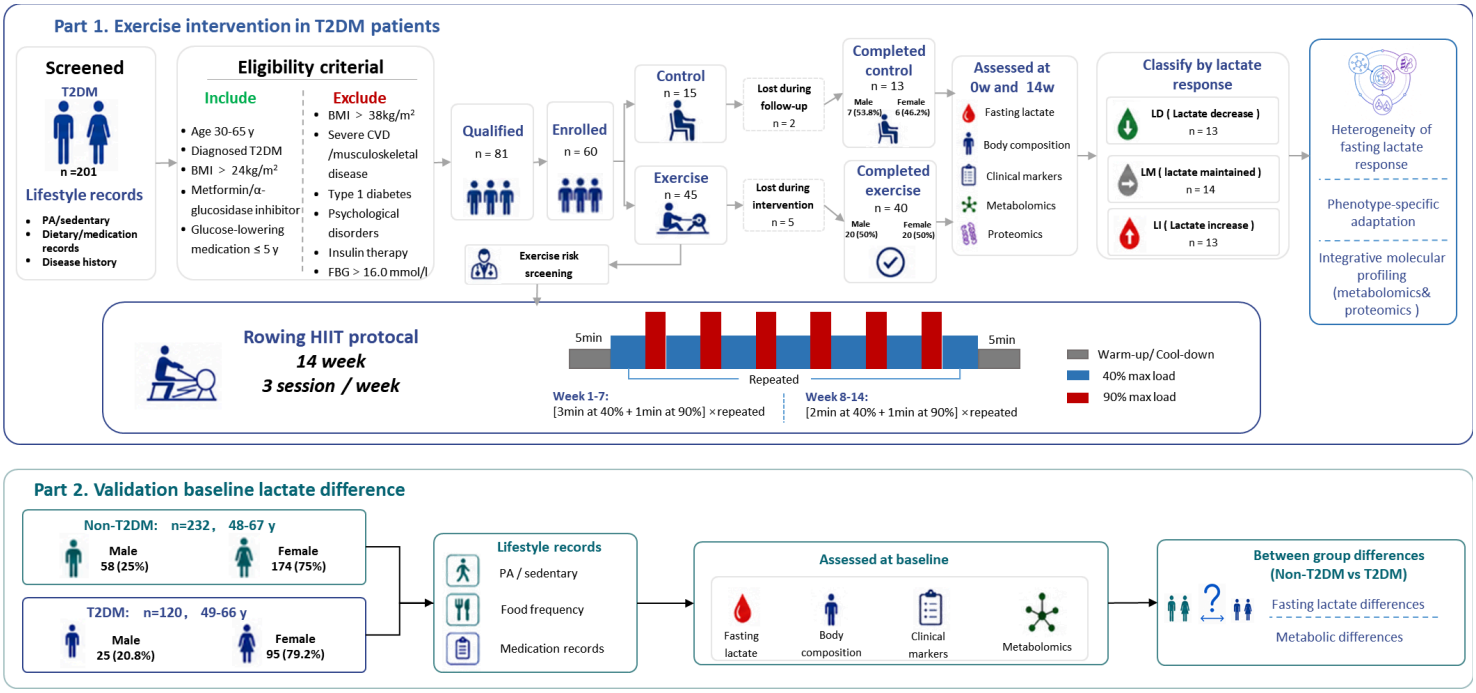


Figure 1

Study design and analytical framework.

A: Patients with T2DM were screened for participation in a 14-week rowing-based HIIT intervention. Eligibility criteria included age 30–65 years, diagnosed T2DM, BMI > 24 kg/m², treatment with metformin or an α-glucosidase inhibitor, and medication history ≤ 5 years. Exclusion criteria included BMI > 38 kg/m², severe cardiovascular or musculoskeletal disease, type 1 diabetes, psychological disorders, insulin therapy and fasting blood glucose > 16.0 mmol/L where applicable. Among 201 screened patients with T2DM, 81 met the eligibility criteria and 60 agreed to enroll. Finally, 40 exercise participants (50.0% men and 50.0% women) and 13 non-exercise controls (53.8% men and 46.2% women) completed all assessments. Fasting lactate and CGM data were assessed at baseline and week 14. Participants in the exercise group were classified into lactate response phenotypes according to the 0–14-week change in fasting lactate: lactate decrease (LD, n = 13), lactate minimal change (LM, n = 14) and lactate increase (LI, n = 13). Within-subject changes in lactate, clinical markers, metabolomics and proteomics were analysed by lactate response phenotype. The rowing HIIT protocol was performed three sessions per week for 14 weeks and included warm-up/cool-down periods, low-intensity rowing at 40% maximal load and high-intensity intervals at 90% maximal load.

B: An independent baseline validation cohort was used to compare lactate and metabolic differences between non-T2DM controls and patients with T2DM. The validation cohort included non-T2DM controls (n = 232; 58 men [25.0%] and 174 women [75.0%]; age range, 48–67 years) and patients with T2DM (n = 120; 25 men [20.8%] and 95 women [79.2%]; age range, 49–66 years). Lifestyle records, including physical activity, sedentary behaviour, food frequency and medication records, were collected. Fasting lactate, clinical markers and serum metabolomic profiles were assessed at baseline to evaluate between-group differences in lactate-associated metabolism.

BMI, body mass index; CGM, continuous glucose monitoring; CVD, cardiovascular disease; FBG, fasting blood glucose; HIIT, high-intensity interval training; PA, physical activity; T2DM, type 2 diabetes mellitus.

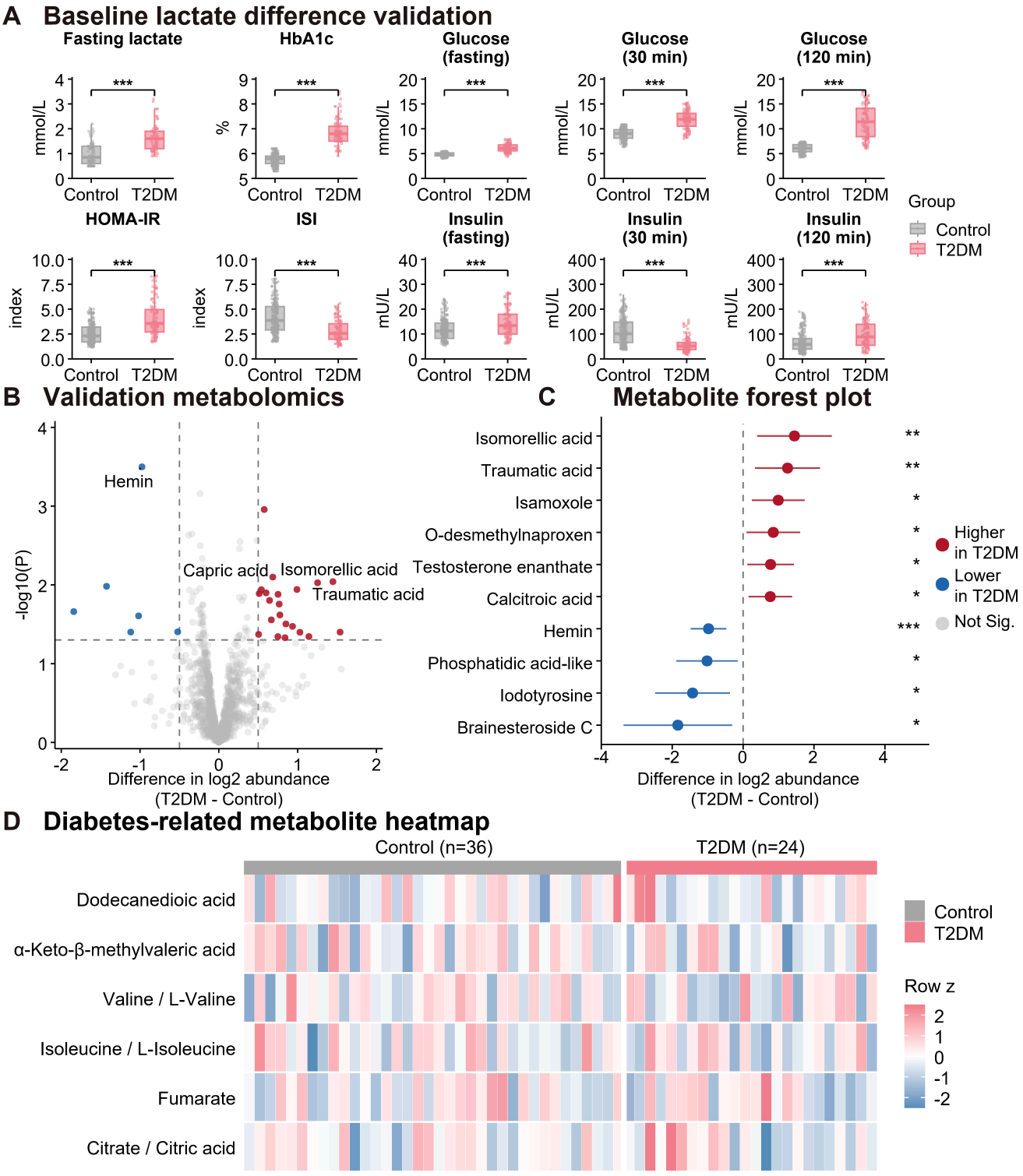


Figure 2

Baseline clinical and metabolomic differences between non-T2DM controls and patients with T2DM

(A) Baseline clinical markers in non-T2DM controls and patients with T2DM. Data are shown as individual values with box plots. Between-group comparisons were performed using Wilcoxon rank-sum tests. ***P < 0.001.

(B) Volcano plot of baseline serum metabolomic differences between patients with T2DM and non-T2DM controls. The x-axis shows the difference in log2 abundance, calculated as T2DM minus Control, and the y-axis shows −log10(P). Red, blue and

grey points indicate features higher in T2DM, lower in T2DM and non-significant features, respectively.

(C) Forest plot of representative top-ranked annotated metabolite features from the baseline comparison. Points indicate log2 abundance differences, horizontal lines indicate confidence intervals, and P values are shown on the right.

(D) Pathway-guided heatmap of selected metabolites related to lactate-connected substrate handling, including central carbon/TCA metabolism, BCAA-related metabolism and dicarboxylate/ω-oxidation-related lipid handling. Values are shown as row-scaled z-scores.

HOMA-IR, homeostasis model assessment of insulin resistance; ISI, insulin sensitivity index; T2DM, type 2 diabetes mellitus; TCA, tricarboxylic acid cycle. Metabolite identities are based on untargeted LC–MS annotation and should be interpreted as putative unless validated by targeted methods. BCAA, branched-chain amino acid.

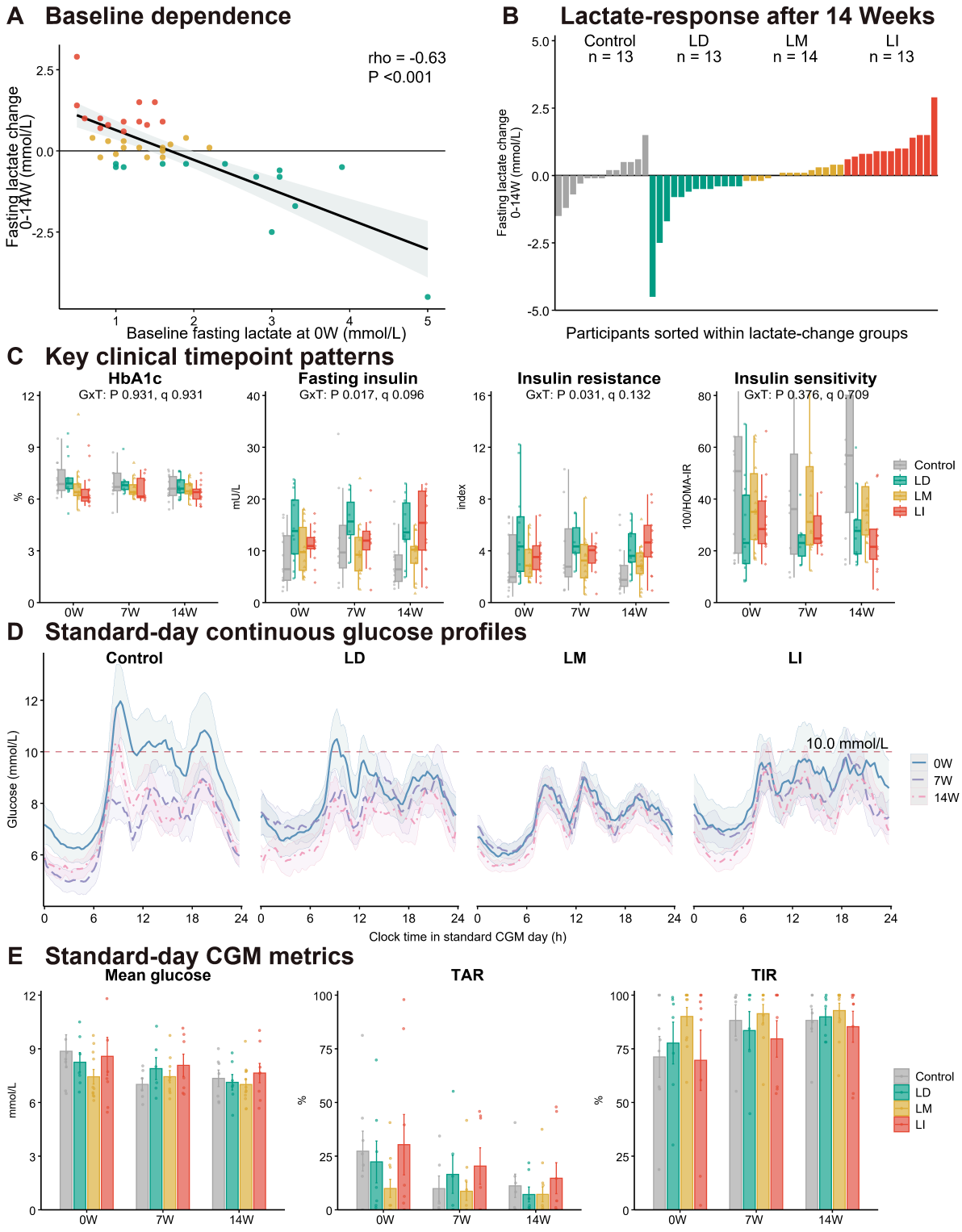


Figure 3

Exercise intervention induces fasting lactate-response heterogeneity and distinct clinical trajectories during the 14-week intervention.

(A) Association between baseline fasting lactate and 0–14-week fasting lactate change among exercised participants. Green, yellow and red represent the LD, LM and LI groups, respectively.

(B) Waterfall plot showing individual 0–14-week fasting lactate changes and separation of lactate-response groups.

(C) Longitudinal patterns of HbA1c, fasting insulin, HOMA-IR and insulin sensitivity. Group-by-time effects are shown for each variable.

(D) Standard-day CGM profiles across baseline, week 7 and week 14. The dashed line indicates the conventional hyperglycaemia threshold of 10.0 mmol/L.

(E) CGM-derived metrics, including mean glucose, TAR and TIR, across the intervention.

CGM, continuous glucose monitoring; HIIT, high-intensity interval training; HOMA-IR, homeostasis model assessment of insulin resistance; LD, lactate decreased; LI, lactate increased; LM, lactate maintained; TAR, time above range; T2DM, type 2 diabetes mellitus; TIR, time in range.

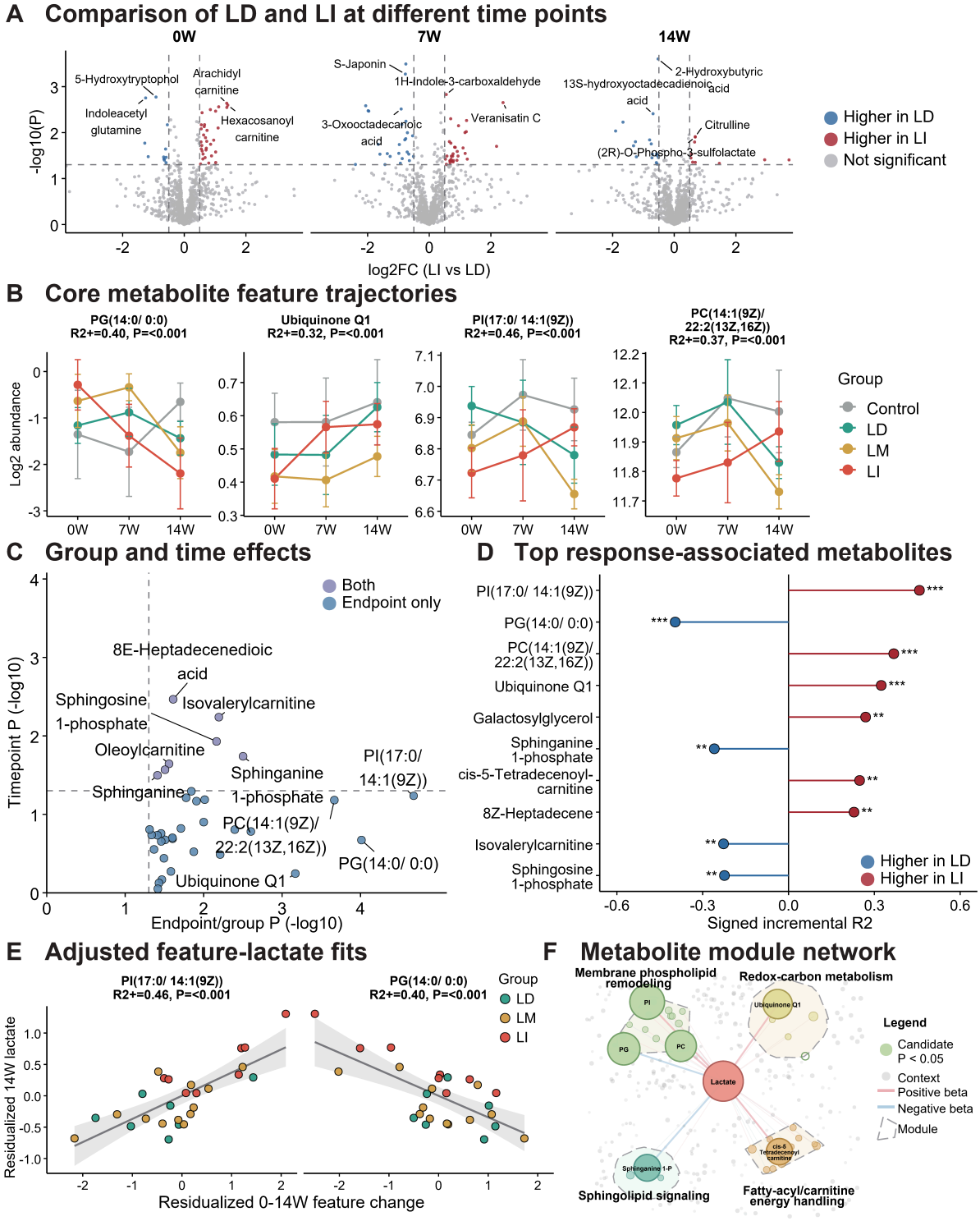


Figure 4

Metabolomic features associated with lactate-response phenotypes

(A) Timepoint-wise LD–LI comparisons of serum metabolite features at baseline, week 7 and week 14. Volcano plots show log2 fold change, calculated as LI minus LD, and −log10(P) from Welch's tests. Red, blue and grey points indicate features higher in LI, higher in LD and non-significant features, respectively.

(B) Trajectories of representative lactate-associated metabolite features across Control, LD, LM and LI groups. Points indicate group means of log2 abundance, and error bars indicate standard error. Facet labels show incremental R^2 and P values from adjusted endpoint models assessing associations between 0–14-week feature changes and week-14 fasting lactate after adjustment for baseline fasting lactate and age.

(C) Integrated endpoint and timepoint evidence for selected metabolite features. Dashed lines indicate nominal P = 0.05.

(D) Top response-associated metabolite features ranked by signed incremental R^2 from adjusted endpoint models. Positive values indicate features positively associated with week-14 fasting lactate, whereas negative values indicate inverse associations.

(E) Adjusted feature–lactate fits for representative metabolite features.

(F) Functional module layout of lactate-associated metabolite features. Candidate metabolites were organized into membrane phospholipid remodelling, sphingolipid signalling, fatty-acyl/carnitine energy handling and redox-carbon metabolism modules. Faint background nodes indicate QC-passed context features and are not interpreted individually. Edge colour indicates the direction of the adjusted beta coefficient.

LD, lactate decreased; LI, lactate increased; LM, lactate maintained; log2FC, log2 fold change; R^2, coefficient of determination. Metabolite identities are based on untargeted LC–MS annotation and should be interpreted as putative unless validated by targeted methods. QC, quality control; R^2+ indicates full model R^2 minus base model R^2.

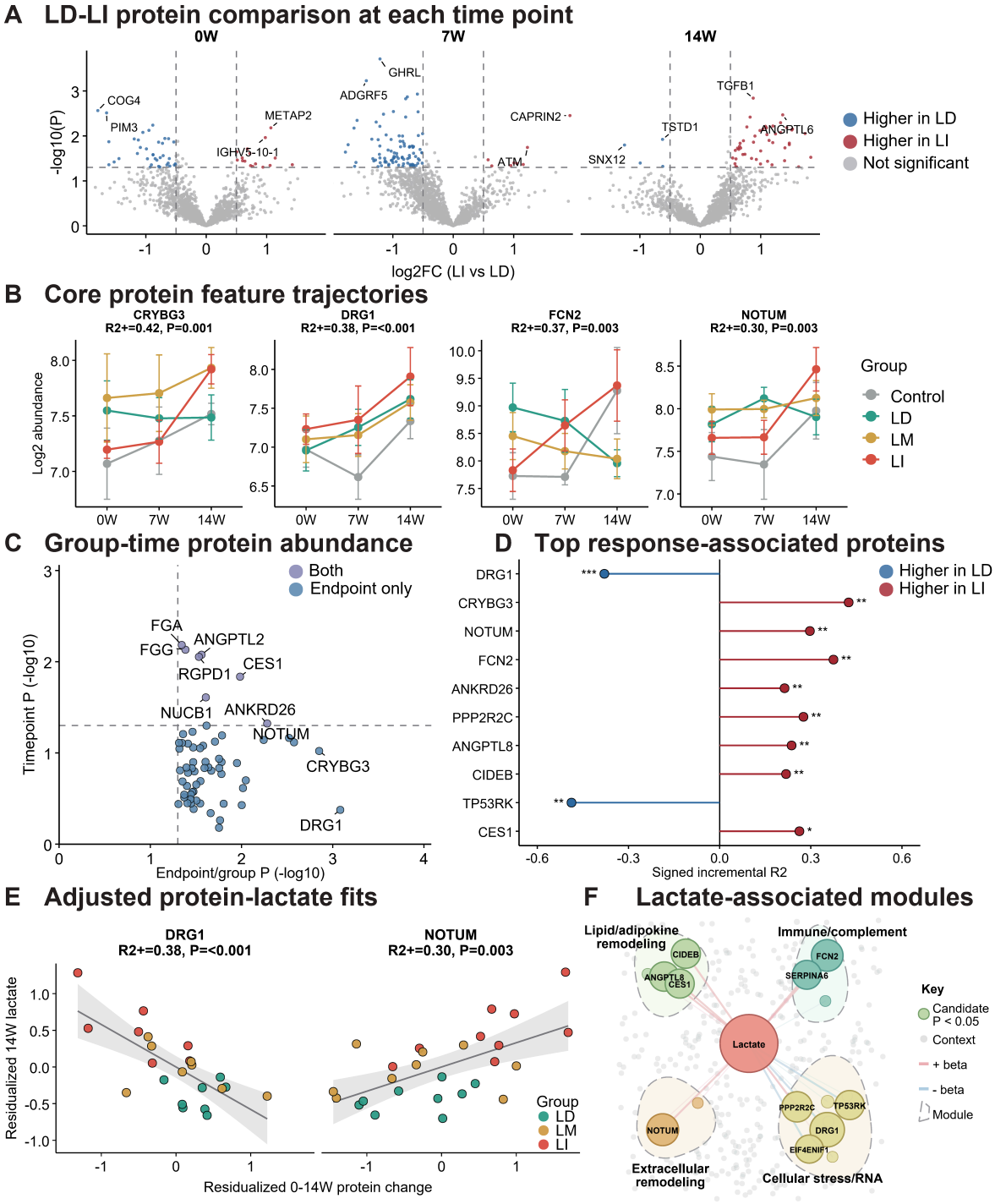


Figure 5

Proteomic features associated with lactate-response phenotypes

(A) Timepoint-wise LD–LI comparisons of serum protein features at baseline, week 7 and week 14. Volcano plots show log2 fold change, calculated as LI minus LD, and −log10(P) from Welch's tests. Red, blue and grey points indicate features higher in LI, higher in LD and non-significant features, respectively.

(B) Trajectories of representative lactate-associated protein features across Control, LD, LM and LI groups. Points indicate group means of log2 abundance, and error bars indicate standard error. Facet labels show incremental R^2 and P values from adjusted endpoint models assessing associations between 0–14-week protein feature changes and week-14 fasting lactate after adjustment for baseline fasting lactate, age, sex, BMI and drug-class count.

(C) Integrated endpoint and timepoint evidence for selected protein features. Dashed lines indicate nominal P = 0.05.

(D) Top response-associated protein features ranked by signed incremental R^2 from adjusted endpoint models. Positive values indicate proteins positively associated with week-14 fasting lactate, whereas negative values indicate inverse associations

(E) Adjusted protein–lactate fits for representative protein features.

(F) Functional module layout of lactate-associated protein features. Candidate proteins were organized into lipid/adipokine remodelling, immune/complement activity, extracellular remodelling and cellular stress/RNA modules. Context proteins and QC-passed background proteins provide visual context and are not interpreted as individual mechanistic nodes. Edge colour indicates the direction of the adjusted beta coefficient.

BMI, body mass index; LD, lactate decreased; LI, lactate increased; LM, lactate maintained; log2FC, log2 fold change; R^2, coefficient of determination. Protein features are reported at the feature level with corresponding gene symbols where available. These analyses were exploratory. QC, quality control. R^2+ indicates full model R^2 minus base model R^2.

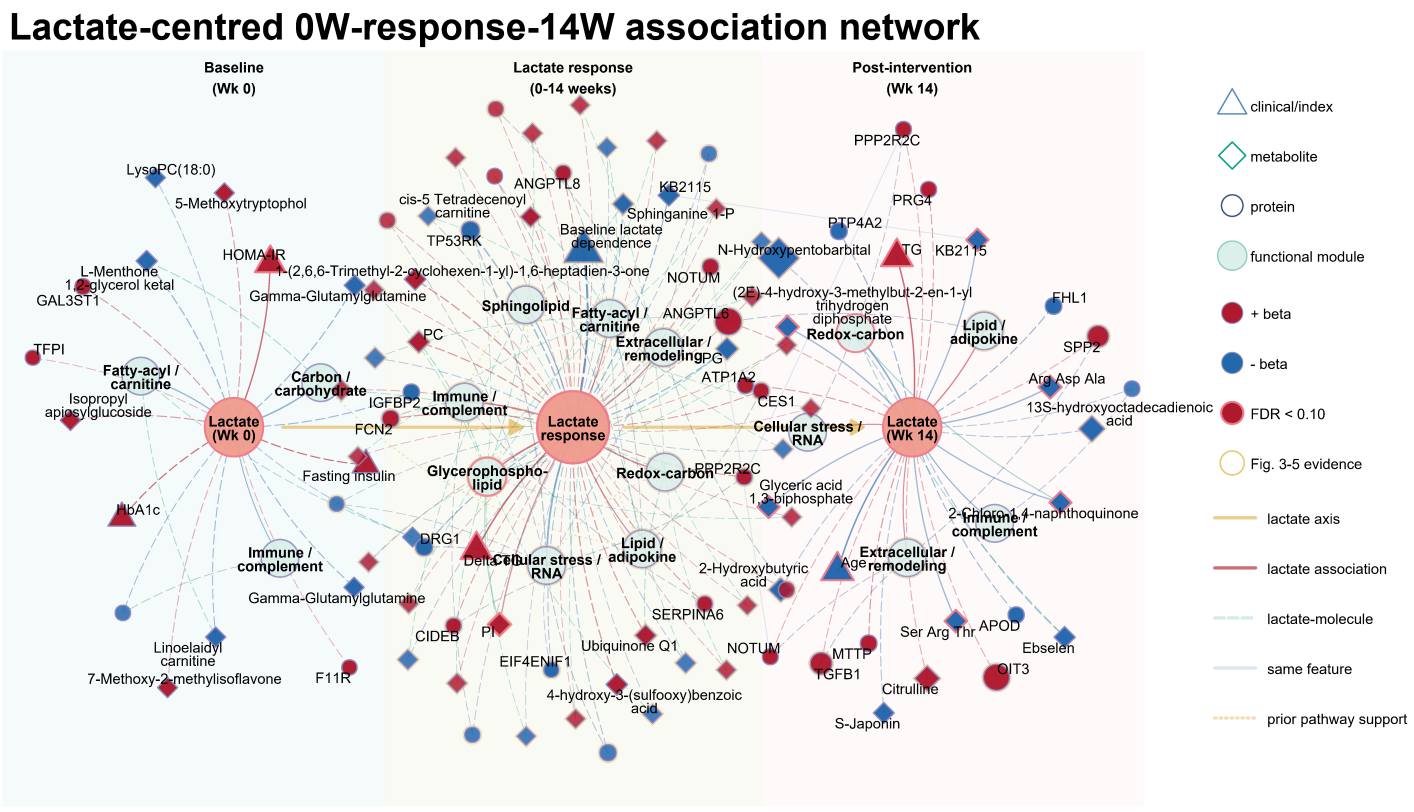


Figure 6

Time-layered lactate-centred association network from baseline to week 14.

Exploratory lactate-centred network summarizing clinical, metabolomic and proteomic associations around fasting lactate at baseline, adjusted lactate response over 0–14 weeks and post-intervention fasting lactate at week 14. The three shaded

regions indicate baseline, lactate-response and post-intervention layers. Central lactate nodes are connected along the temporal lactate axis. Node shape denotes data class: triangles, clinical indices; diamonds, metabolites; circles, proteins; and large pale circles, functional modules. Node colour indicates the direction of association where available, with red representing positive beta coefficients and blue representing negative beta coefficients. Node border indicates statistical support, including FDR < 0.10 or nominal evidence. Pale gold halos indicate features traceable to Fig. 3–5 evidence. Edges indicate lactate associations, lactate–molecule links, module–feature membership, repeated features across time layers or prior pathway support. The network is pathway-guided and hypothesis-generating and should not be interpreted as evidence of causal mediation or validated mechanisms.

BMI, body mass index; FDR, false discovery rate; HbA1c, glycated haemoglobin; HIIT, high-intensity interval training; HOMA-IR, homeostasis model assessment of insulin resistance; TG, triglycerides.

Supplementary Files

This is a list of supplementary files associated with this preprint. Click to download.

- Supplementarymaterial.docx
- GA.png